Analytical Investigation of the Dynamics of Tethered Constellations in Earth Orbit (Phase II)

Contract NAS8-36606

Quarterly Report # 10

For the period 1 July 1987 through 30 September 1987

Principal Investigator

Dr. Enrico C. Lorenzini

Co-Investigators

Mr. David A. Arnold
Dr. Mario Cosmo
Dr. Mario D. Grossi
Dr. Gordon E. Gullahorn

October 1987

Prepared for
National Aeronautics and Space Administration
Marshall Space Flight Center, Alabama 35812

Smithsonian Institution
Astrophysical Observatory
Cambridge, Massachusetts 02138

CONTENTS

CONTENTS (Cont.)

Summary

This Quarterly Report deals with the following topics:

Simulation of two short distance crawling maneuvers of the elevator both with and without environmental perturbations acting upon the system. These simulation runs have been done in order to provide results useful for the interpretation of the data from the tests, on the ground, of a scaled down engineering model of the elevator. In these simulation runs the elevator crawls along the tether in accordance to the newly developed mirror image motion control law (*MIMCL*).

Simulation of a typical 4-km-long maneuver of the elevator in accordance to the *MIMCL*. The results from this simulation run have been compared to those obtained by adopting the modified hyperbolic tangent control law (*MHTCL*).

Development of a preprocessor for setting up the initial conditions of a tethered system with L platforms, M longitudinal dampers and N lumped masses (platforms plus tether beads). A short test run of our 4-platform system with 3 longitudinal dampers and 10 lumped mass without any perturbation acting upon the system is also illustrated.

In support of the Tether Applications Working Group, SAO: (a) is preparing a catalog of tether simulations; (2) has prepared a set of simulator test cases, obtained results from SKYHOOK, and solicited results from simulators at other institutions; (3) prepared a paper on a specific analytic solution.

Figure Captions

Figures 1a-1m. System's dynamic response obtained by adopting the mirror image motion control law (*MIMCL*) for a short distance crawling maneuver of the elevator. All the environmental perturbations are acting upon the system. The control parameters are as follows: total distance travelled $\Delta\ell_{cT}$ = 2 m, time constant $1/\alpha$ = 400 sec, shape parameter γ = 4 and constant-velocity-parameter Y = 0.8.

Figures 2a-2m. System's dynamic response under the same conditions of Figures 1 but without any environmental perturbation acting upon the system.

Figures 3a-3q. System's dynamic response under the same conditions of Figures 1 except for the total travelled distance $\Delta\ell_{cT}$ that is equal to 9.75 m.

Figures 4a-4m. System's dynamic response under the same conditions of Figures 3 but without any environmental perturbation acting upon the system.

Figures 5a-5m. System's dynamic response under the same conditions of Figures 1 except for the control parameters which are as follows: $\Delta\ell_{cT}$ = 4 km, $1/\alpha$ = 1000 sec, γ = 4 and Y = 0.8.

Figures 6a-6m. System's dynamic response under the same conditions of Figures 5 except that only the J_2-perturbations are acting upon the system.

Figure 7. Schematic of the lumped mass model.

Figures 8a-8d. Dynamic response of a 4-platform tethered system with 3 longitudinal dampers and 10 lumped masses (4 platforms plus 6 tether beads) with no environmental perturbations. The space station coincides, at time equal to zero, with the system *CM* and with the origin of the orbiting reference frame. The system is initially aligned with *LV*.

Figures 9a-9d. Dynamic response of a 4-platform system as in Figures 6 except that the space station coincides, at time equal to zero, with the system *CO* and with the origin of the orbiting reference frame.

1.0 INTRODUCTION

This is the tenth Quarterly Report submitted by SAO under contract NAS8-36606, "Analytical Investigation of the Dynamics of Tethered Constellations in Earth Orbit (Phase II)," Dr. Enrico C. Lorenzini, PI. This reports covers the period from 1 July 1987 through 30 September 1987.

2.0 TECHNICAL ACTIVITY DURING REPORTING PERIOD AND PROGRAM STATUS

2.1 Mirror Image Motion Control Law For The Space Elevator

The modified hyperbolic tangent with constant velocity phase control law (*MHTCL*) provides smooth and relatively rapid crawling maneuvers of the elevator. The *MHT* control law, however, is not symmetrical; specifically the deceleration phase is slower than the acceleration phase. Since the acceleration level on board the elevator is the driver for the selection of the control parameters, the time constant is determined by the maximum acceleration during the acceleration phase. Consequently the deceleration phase is slower than necessary. In order to speed up the maneuver Swenson and Rupp have proposed to make the *MHT* control law symmetrical by replacing the deceleration phase with the mirror image of the acceleration phase. The new control law has been called mirror image motion control law (*MIMCL*).

The three phases of the *MIMCL* are therefore as follows:

1. Acceleration Phase

$$\Delta\ell_c = \Delta\ell_c' \left[\tanh(\alpha t)\right]^{\gamma} \qquad t < t_A \tag{1.1}$$

2. Constant Velocity Phase

$$\Delta\ell_c = \Delta\ell_c'\left[\tanh(\alpha t_A)\right]^{\gamma} + \Delta\ell_c'' \frac{t - t_A}{t_B - t_A} \qquad t_A \le t < t_B \tag{1.2}$$

3. Deceleration Phase

$$\Delta\ell_c = \Delta\ell_{cT} - \Delta\ell_c'\left\{\tanh\left[\alpha(t_T - t)\right]\right\}^{\gamma} \qquad t_B \le t \le t_T \tag{1.3}$$

Phases 1 and 2 are like those of the *MHT* control law. The meaning of the symbols in equations (1) is as follows:

$t_A = \frac{1}{\alpha} \sinh^{-1}\sqrt{(\gamma\text{-}1)/2}$	time at which the max. velocity is reached
$t_B = t_A + \Delta\ell_c''/\dot{\ell}_{c,m}$	time at the end of constant-velocity-phase
$t_T = t_A + t_B$	total transit time
$\dot{\ell}_{c,m} = \Delta\ell_c'\alpha\frac{2\gamma}{\gamma+1}\left(\frac{\gamma\text{-}1}{\gamma+1}\right)^{(\gamma-1)/2}$	maximum and constant velocity
$\Delta\ell_{cT}$	total variation of travelled length
$\Delta\ell_c'' = Y\Delta\ell_{cT}$	length travelled at constant speed
$\Delta\ell_c'$	amplitude (length) of the hyperbolic tangent function

Because of the modification of the deceleration phase $\Delta\ell_c'$ is no longer the distance travelled during the acceleration and deceleration phase and $\Delta\ell_c'$ is related to $\Delta\ell_{cT}$ by

$$\Delta\ell_c' = \frac{1-Y}{2\left[(\gamma-1)/(\gamma+1)\right]^{\gamma/2}}\,\Delta\ell_{cT} \tag{2}$$

where Y is equal to $1-X$ of the *MHTCL*. It is worth noticing that the cut-off distance σ is no longer required for the *MIMCL* because the deceleration phase is no longer asymptotic.

If we compare the total transit time of a *MIMCL* to the total transit time of a *MHTCL* with same control parameters we obtain that the *MIMCL* is faster than the *MHTCL*. The fractional gain in travel time is given by

$$\xi = \left(t_{T,MIM} - t_{T,MHT}\right)/t_{T,MIM} \tag{3}$$

By using equations (3), (4) and (5) of Quarterly Report #8 and the expression of t_T for the *MIMCL* we obtain

$$\xi = \frac{\tanh^{-1}\left\{\left[1-\tau/(1-Y)\right]^{1/\gamma}\right\} - 2\sinh^{-1}\sqrt{(\gamma-1)/2}}{2\sinh^{-1}\sqrt{(\gamma-1)/2} + Y(\gamma+1)\sqrt{(\gamma-1)/(\gamma+1)}/\left[\gamma(Y-1)\right]} \tag{4}$$

It is worth noticing that ξ does not depend upon the rate parameter α. For $\gamma = 4$, $1-X = Y = 0.8$ and for a cut-off parameter $\tau = \sigma/\Delta\ell_{cT} = 2.5\times10^{-4}$ (for the *MHTCL*) we obtain that the *MIMCL* is 40% faster than the *MHTCL*.

2.1.1 Short Distance Crawling Maneuvers With Mirror Image Motion Control Law

Experimental tests of an elevator's engineering model are underway at NASA/MSFC, Huntsville, Alabama and at Tri-State University, Angola, Indiana. The tests are performed by means of a frictionless flat table. A scaled down elevator moves over the table on an air cushion. The elevator is allowed to move along a horizontal wire that is fixed to one end of the table and is constrained to move in an idle pulley at the other end of the table. A ballast at the loose end of the wire stretches the wire.

This experimental setup does not reproduce some of the characteristics of the actual space system such as the stiffness (softness would be a more appropriate word) of a tether several kilometers long. In order to reproduce the softness of the space system's tethers the point of attachment of the wire in the experimental setup should be moved according to the same longitudinal motion of the same part of the actual tether in the space system. Other phenomena such as Coriolis forces or gravity gradient forces can be potentially reproduced in the experimental setup by tilting the table around the longitudinal and transverse axes respectively. Tension variations caused by variations of tether temperature can be reproduced, in principle, by controlling the tension of the wire in the experimental setup. This means that the ballast should be replaced by an active control system.

A typical crawling maneuver performed on the experimental setup has a length of 2 m for the flat table at Tri-State University and 384 inches = 9.75 m for the flat table at NASA/MSFC.

Two simulation runs have been performed in order to provide results applicable to the two experiments which are going to take place at Tri-State

University and at NASA/MSFC. Both runs make use of the *MIM* control law with the following control parameters and travelled lengths:

Simulation Ia and Ib

$$\Delta\ell_c = 2m,\ 1/\alpha = 400 \text{ sec},\ \gamma = 4,\ Y = 0.8 \tag{5}$$

Simulation IIa and IIb

$$\Delta\ell_c = 9.75\ m,\ 1/\alpha = 400 \text{ sec},\ \gamma = 4,\ Y = 0.8 \tag{6}$$

Simulations I and II are applicable to the flat tables of Tri-State University and NASA/MSFC respectively. The time constant $1/\alpha = 400$ sec is different from the value of 100 sec initially proposed by Rupp and Swenson in order to reduce the maximum acceleration levels on board the elevator during the crawling.

In the simulation runs Ia and IIa all the external perturbations (drag, thermal and J_2) are acting upon the system. In simulations Ib and IIb no perturbation is acting upon the system. In all the runs the space station is placed at the system *CM* and the elevator starts crawling 1000 sec after the beginning of the simulation.

Figures 1a through 1m show the dynamic response of the system under the conditions of simulations Ia. The usual presentation of the actual and controlled tether length of the elevator has been modified in order to make easier the comparison between the two quantities during the crawling. For this reason the caption along the $y - axis$ of Figure 1a has been changed to "*EL* DISTANCE" (from the space station). The controlled distance is meaningful only after the

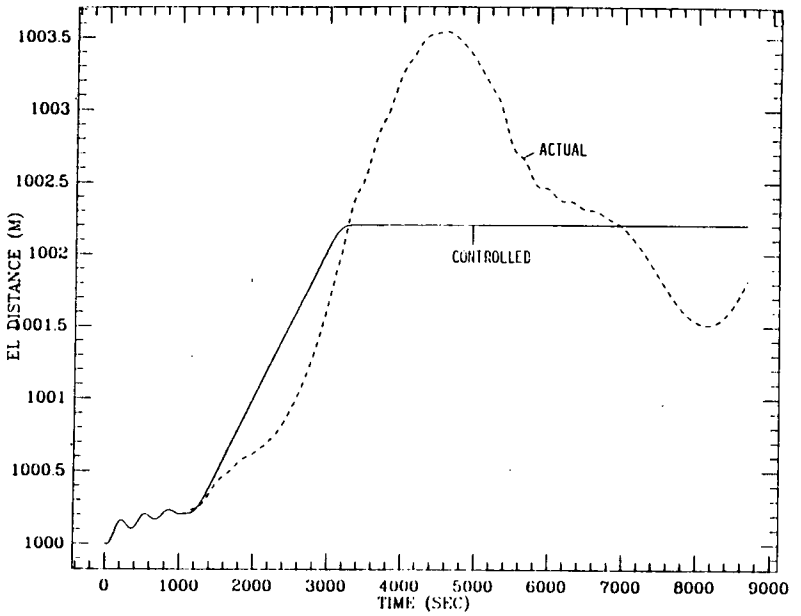

Figure 1a

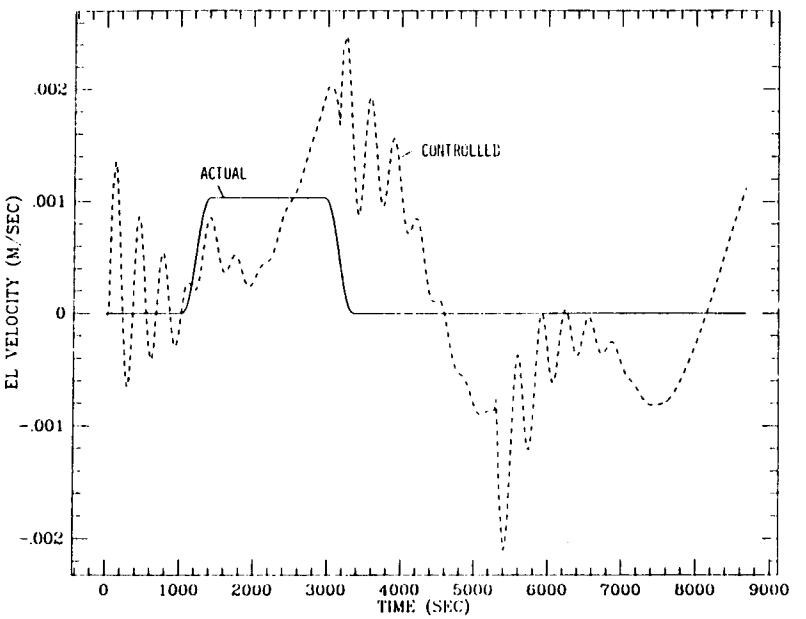

Figure 1b

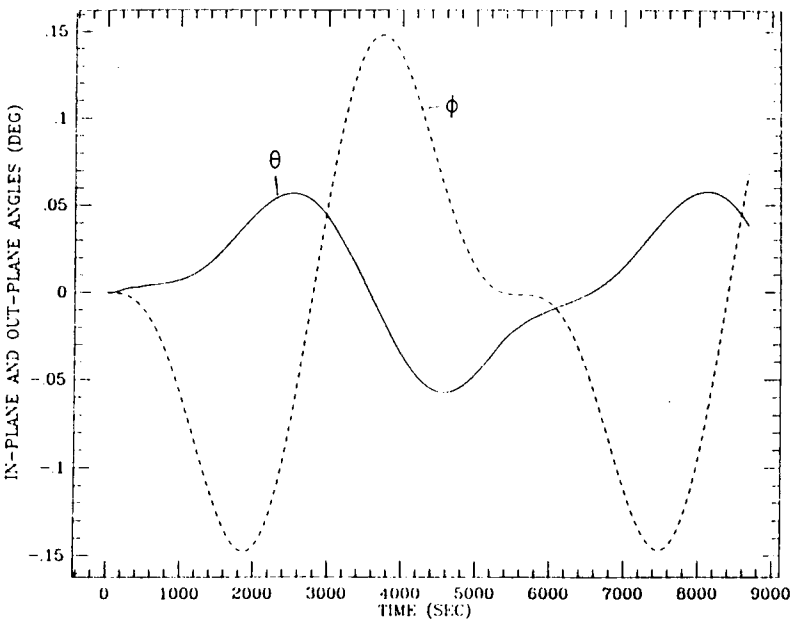

Figure 1c

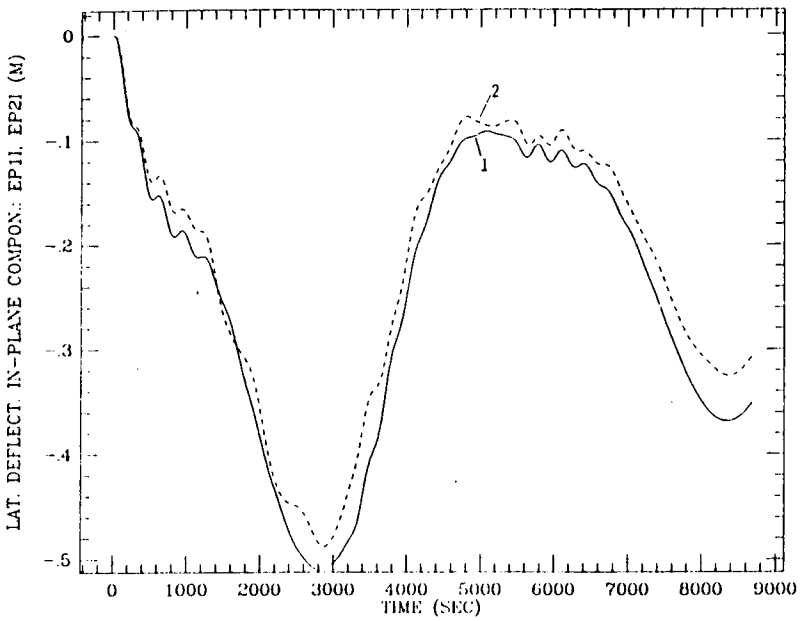

Figure 1d

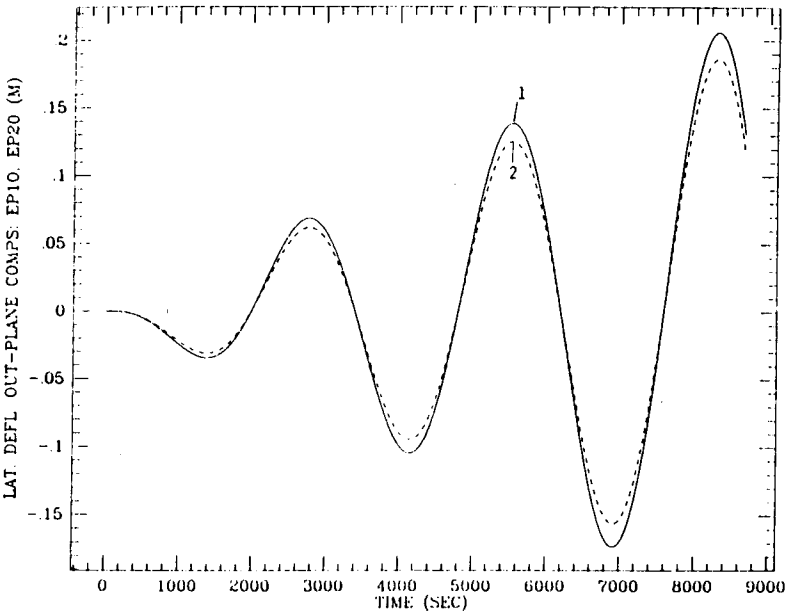

ORIGINAL PAGE IS
OF POOR QUALITY

Figure 1e

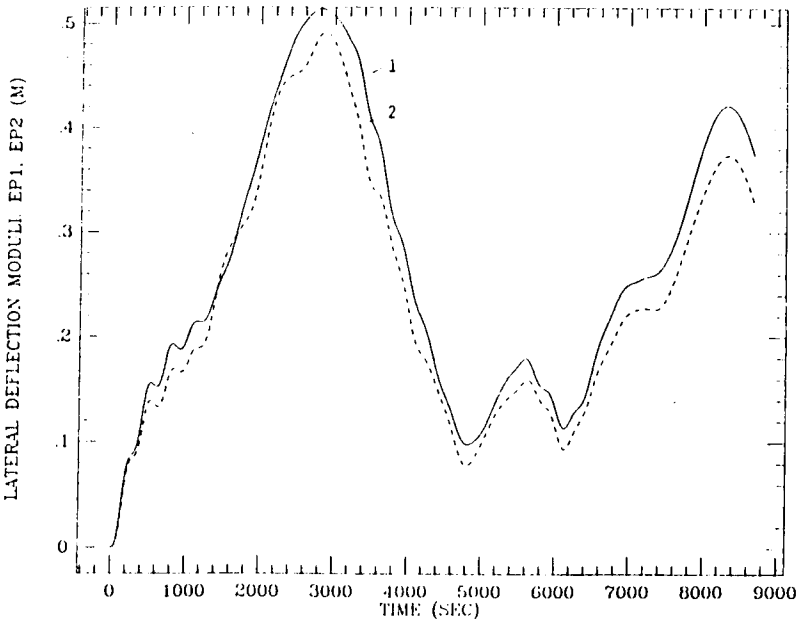

Figure 1f

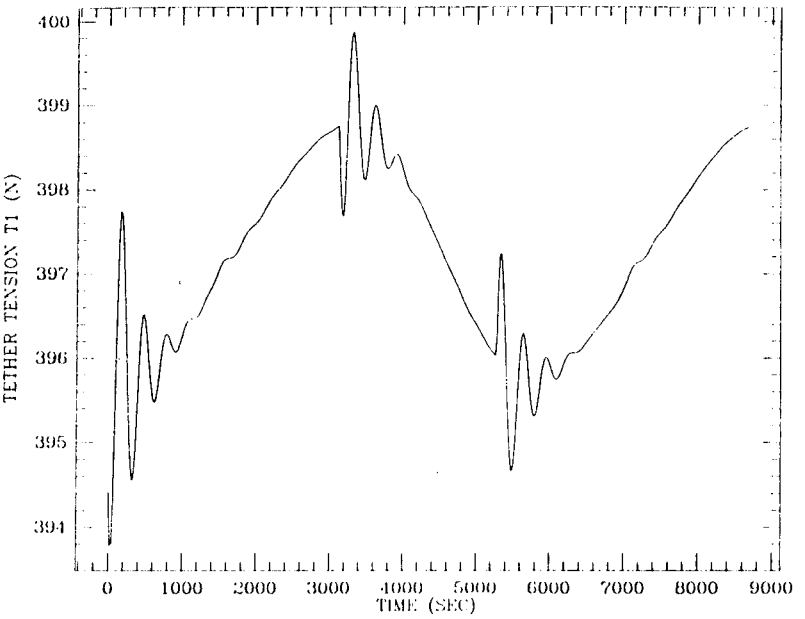

Figure 1g

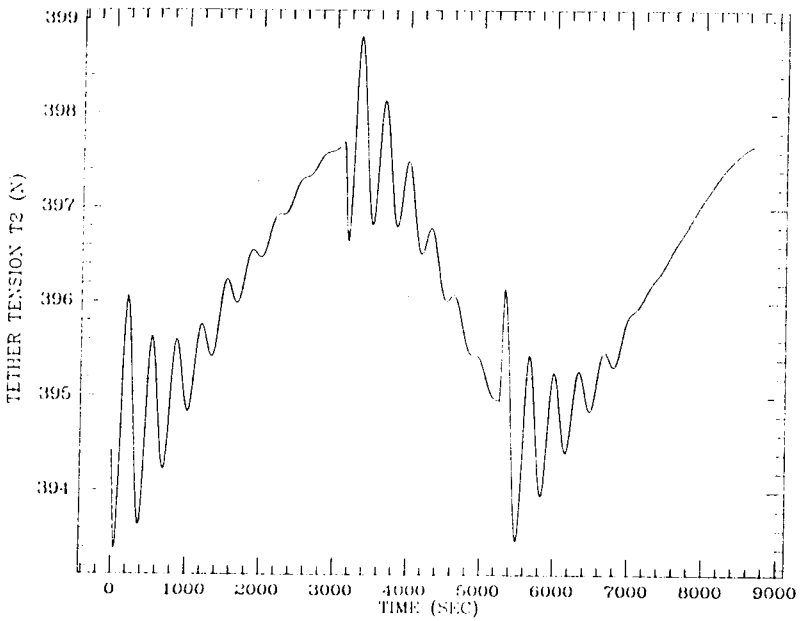

Figure 1h

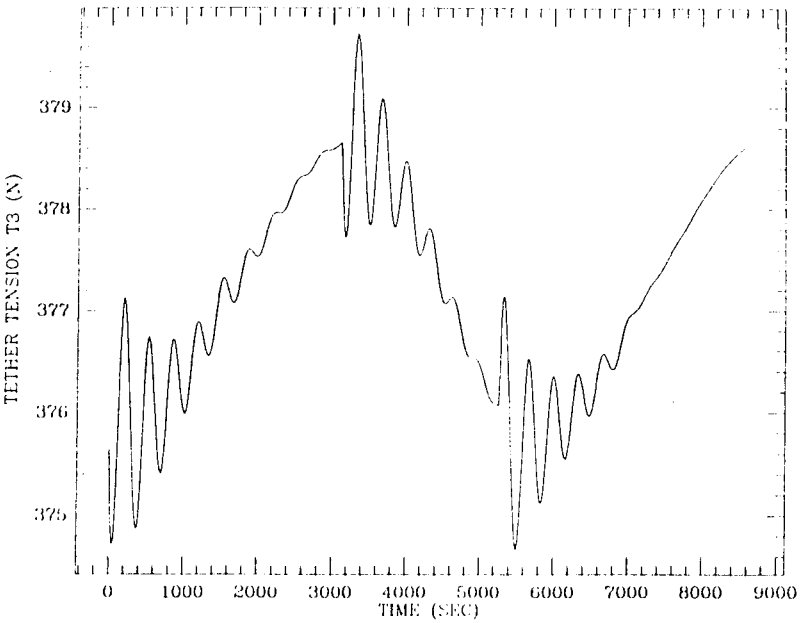

Figure 1i

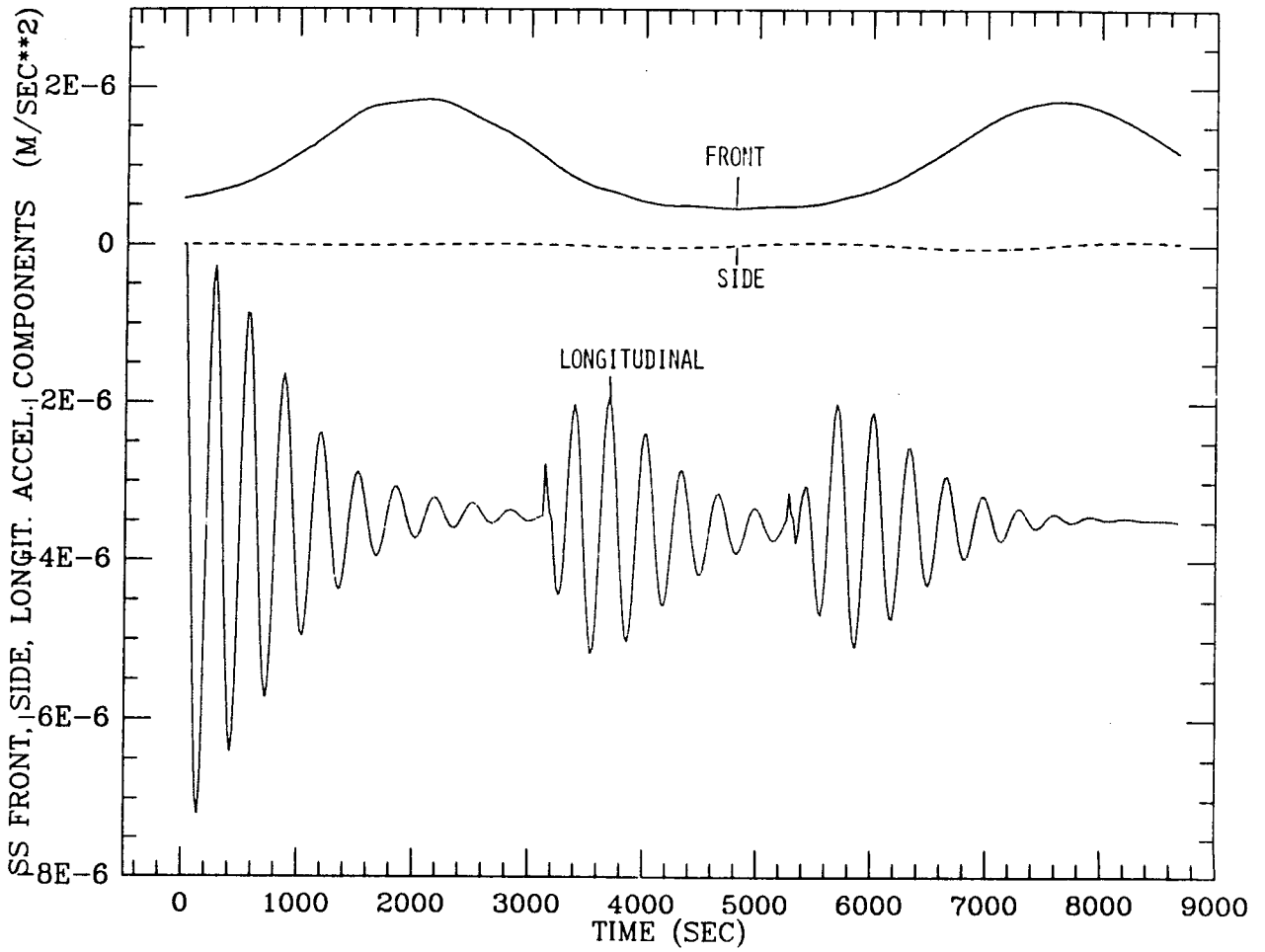
SS FRONT, SIDE, LONGIT. ACCEL. COMPONENTS (M/SEC**2)
2E-6
0
2E-6
4E-6
6E-6
8E-6
FRONT
SIDE
LONGITUDINAL
0
1000
2000
3000
4000
5000
6000
7000
8000
9000
TIME (SEC)

Figure 1j.

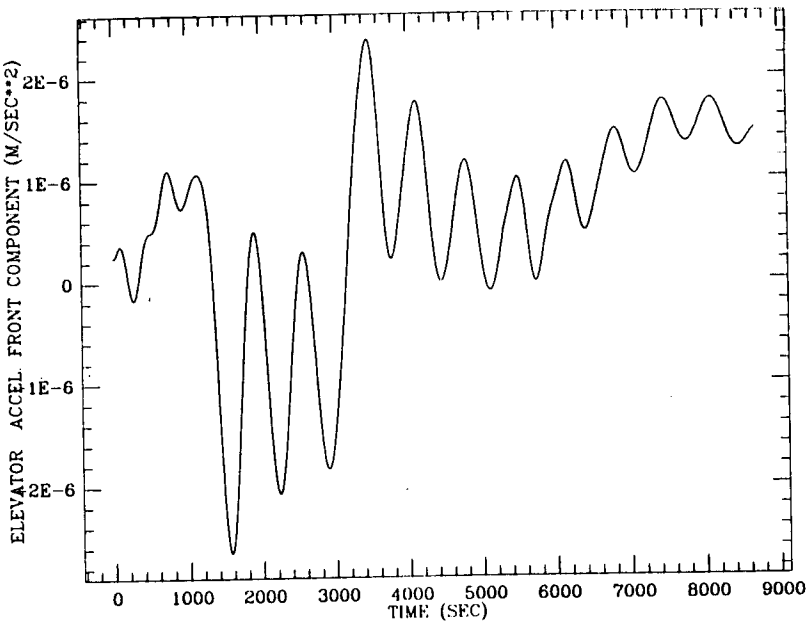

Figure 1k

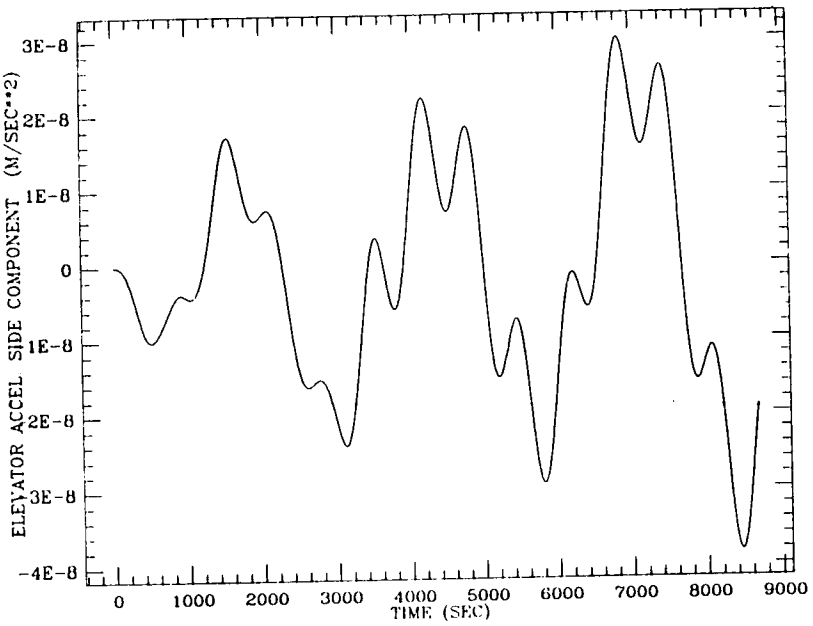

Figure 1ℓ

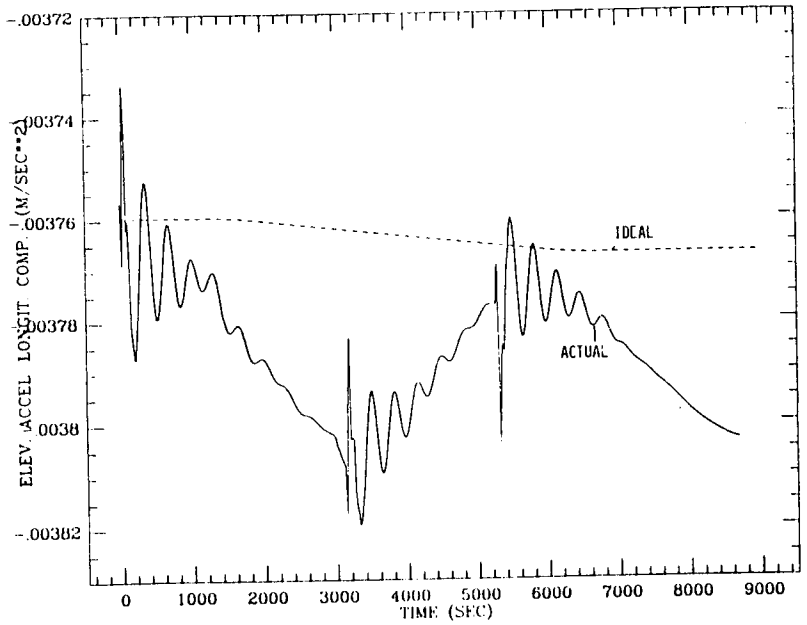

Figure 1m

inception of the elevator's motion and it is set equal to the actual distance at the motion's inception. The controlled distance is provided by the elevator's motion control law and the actual distance differs from the controlled distance because of tether elasticity and the stretch of the longitudinal damper.

Figure 1b shows the controlled and actual velocity of the elevator. The controlled velocity is the derivative of the elevator's motion control law. The controlled velocity is equal to zero before the elevator starts to move. The controlled velocity before the elevator's motion must not be interpreted as the derivative of the controlled distance before the elevator's motion shown in Figure 1a. Such controlled distance is in fact meaningless before the initiation of the motion.

The remaining figures show the libration angles, the lateral deflections of the inner-masses, the tension in the tether segments, the components of the acceleration on board the station and on board the elevator. In particular Figure 1m compares the longitudinal component of the actual acceleration on board the elevator with the ideal acceleration. It is evident from this figure that the acceleration noise, generated primarily by J_2 and thermal disturbances, is greater than the ideal variation of acceleration level during the crawling maneuver. The total travelled distance is too short to produce a variation of acceleration large enough to overcome the noise.

In order to provide results which show the differences in dynamic response between the highly elastic space system and the "stiff" experimental setup we reran the simulation without environmental perturbations. The results of simulation Ib are shown in Figures 2a through 2m which are in the same sequence of the previous set of figures. In Figure 2a it is worth noticing the small

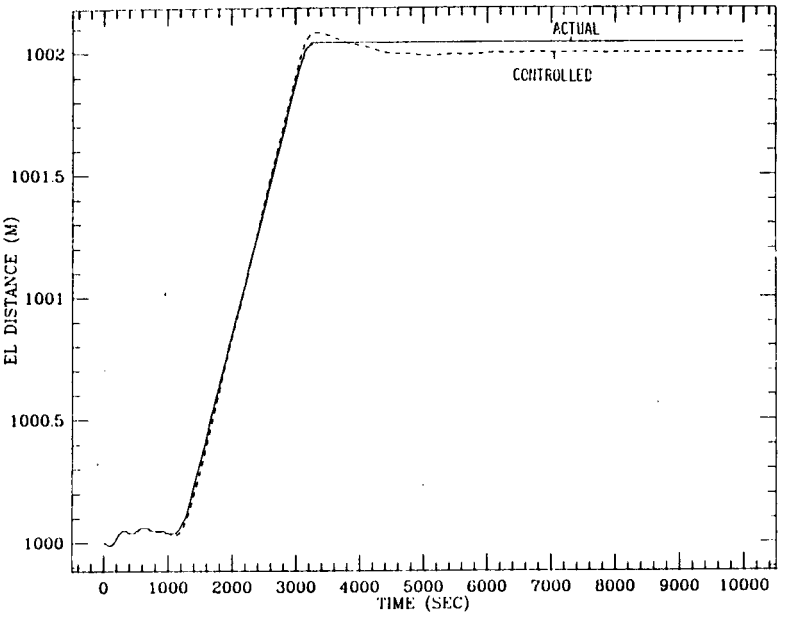

Figure 2a

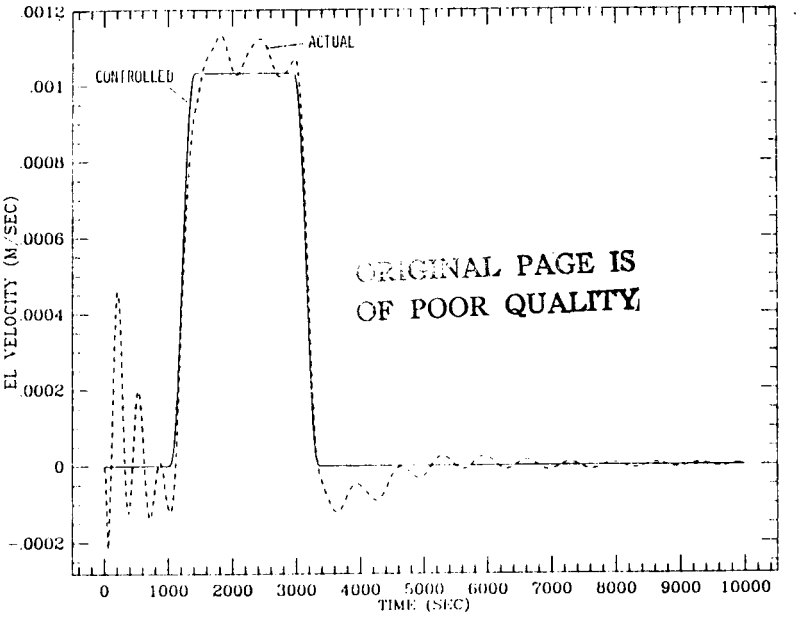

Figure 2b

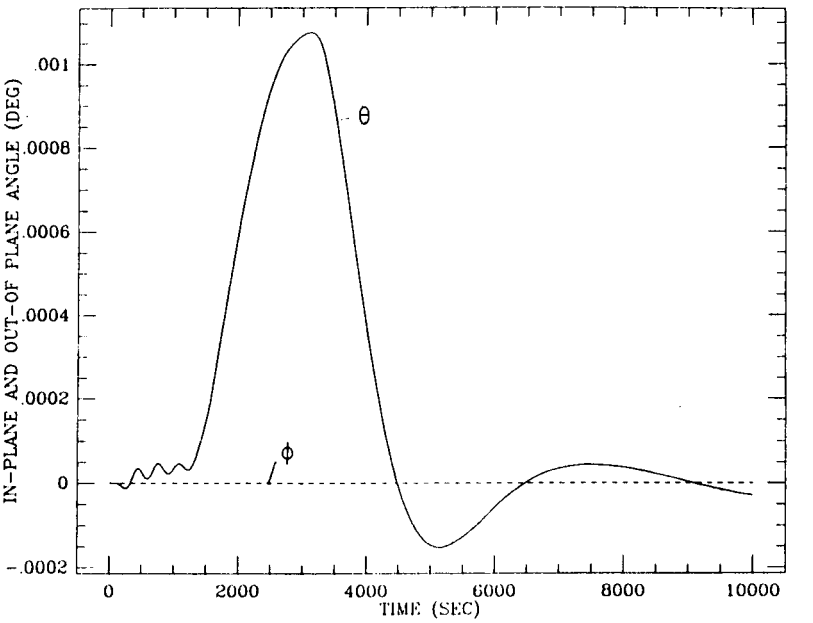

Figure 2c

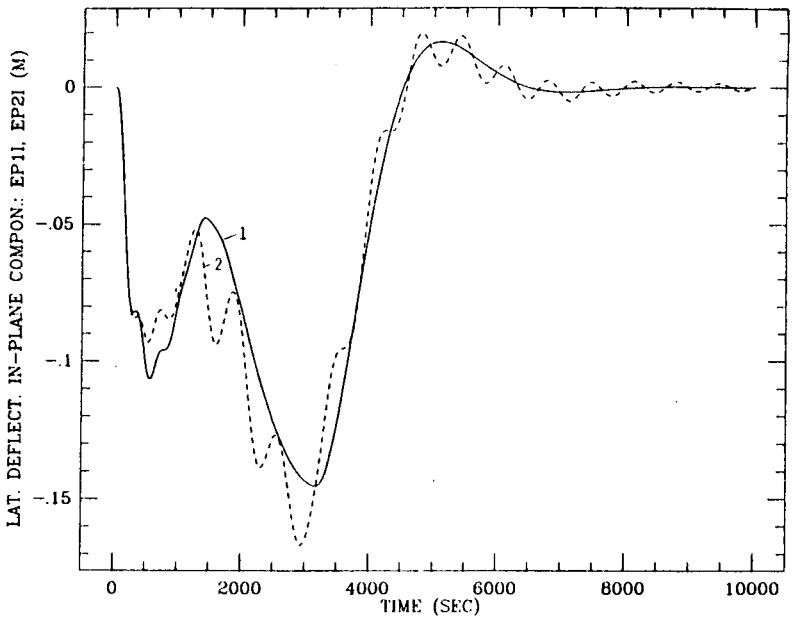

Figure 2d

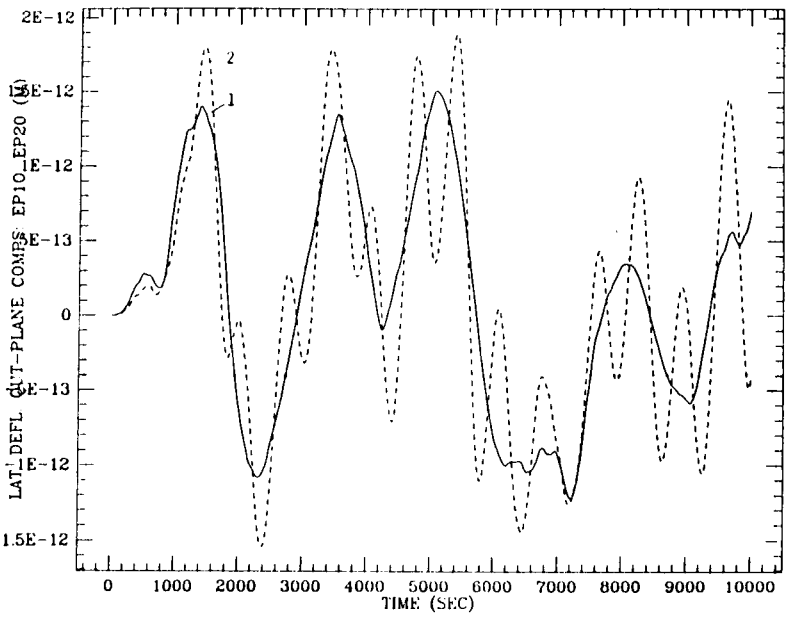

Figure 2e

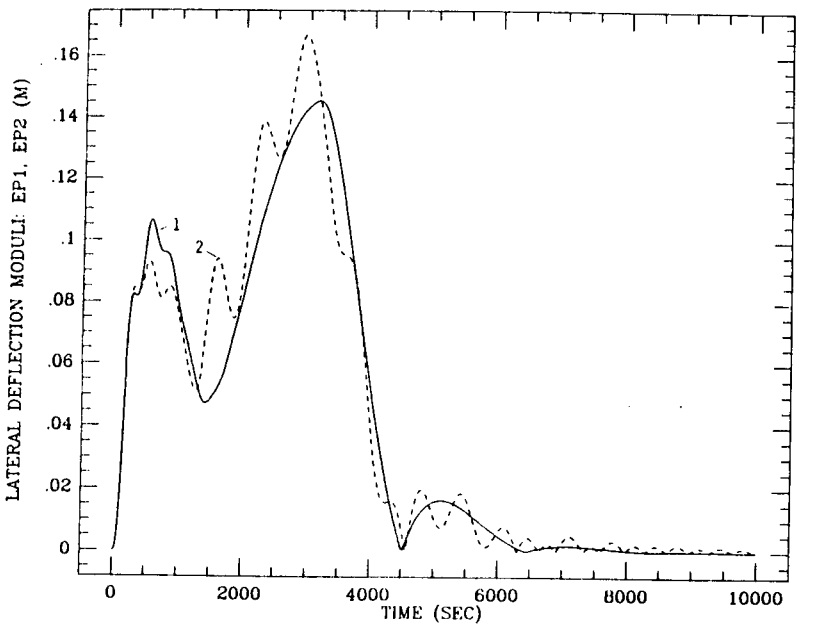

Figure 2f

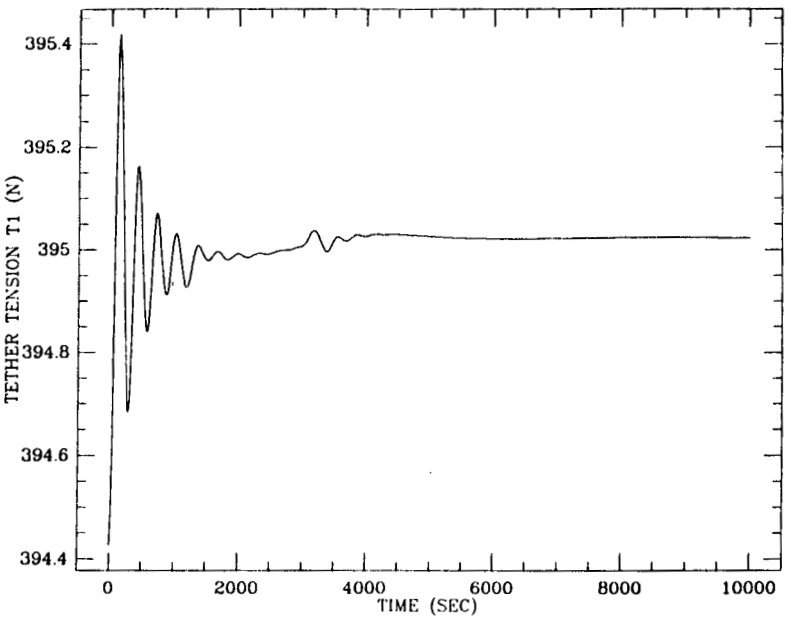

Figure 2g

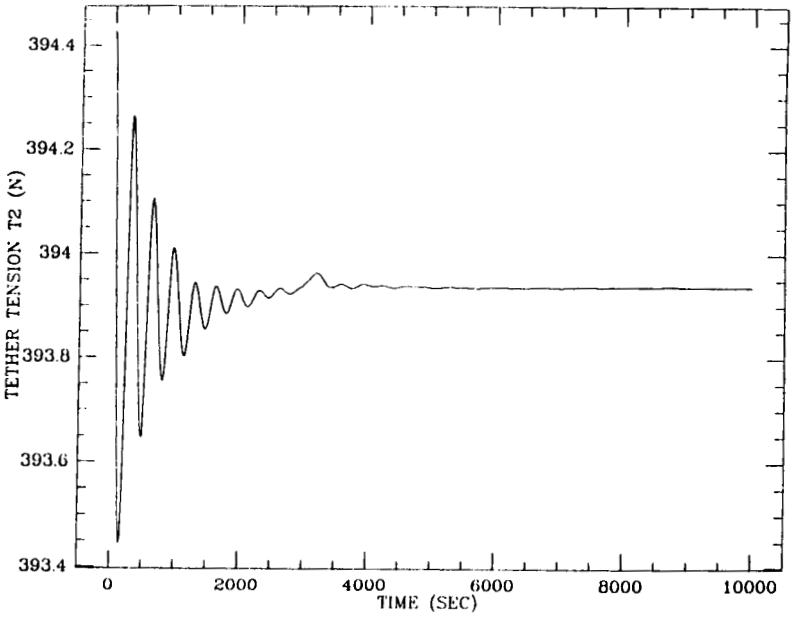

Figure 2h

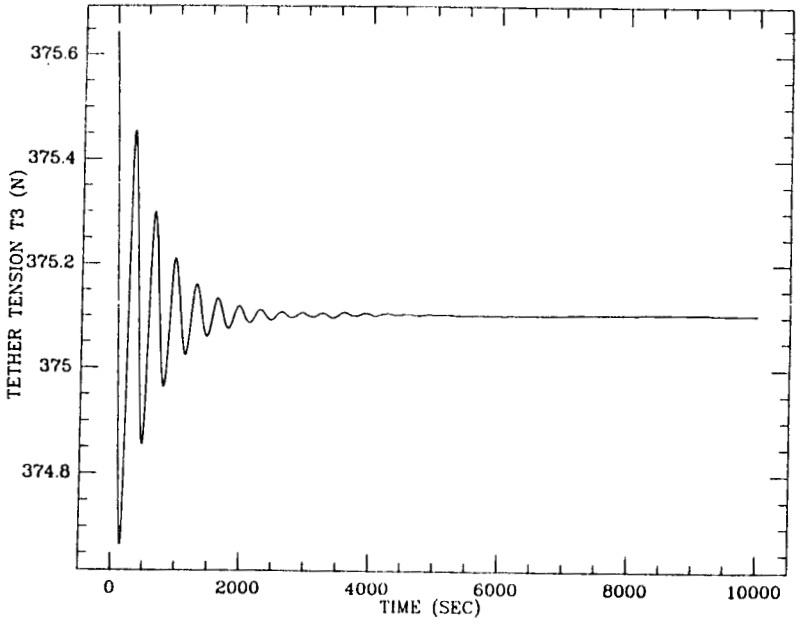

Figure 2i

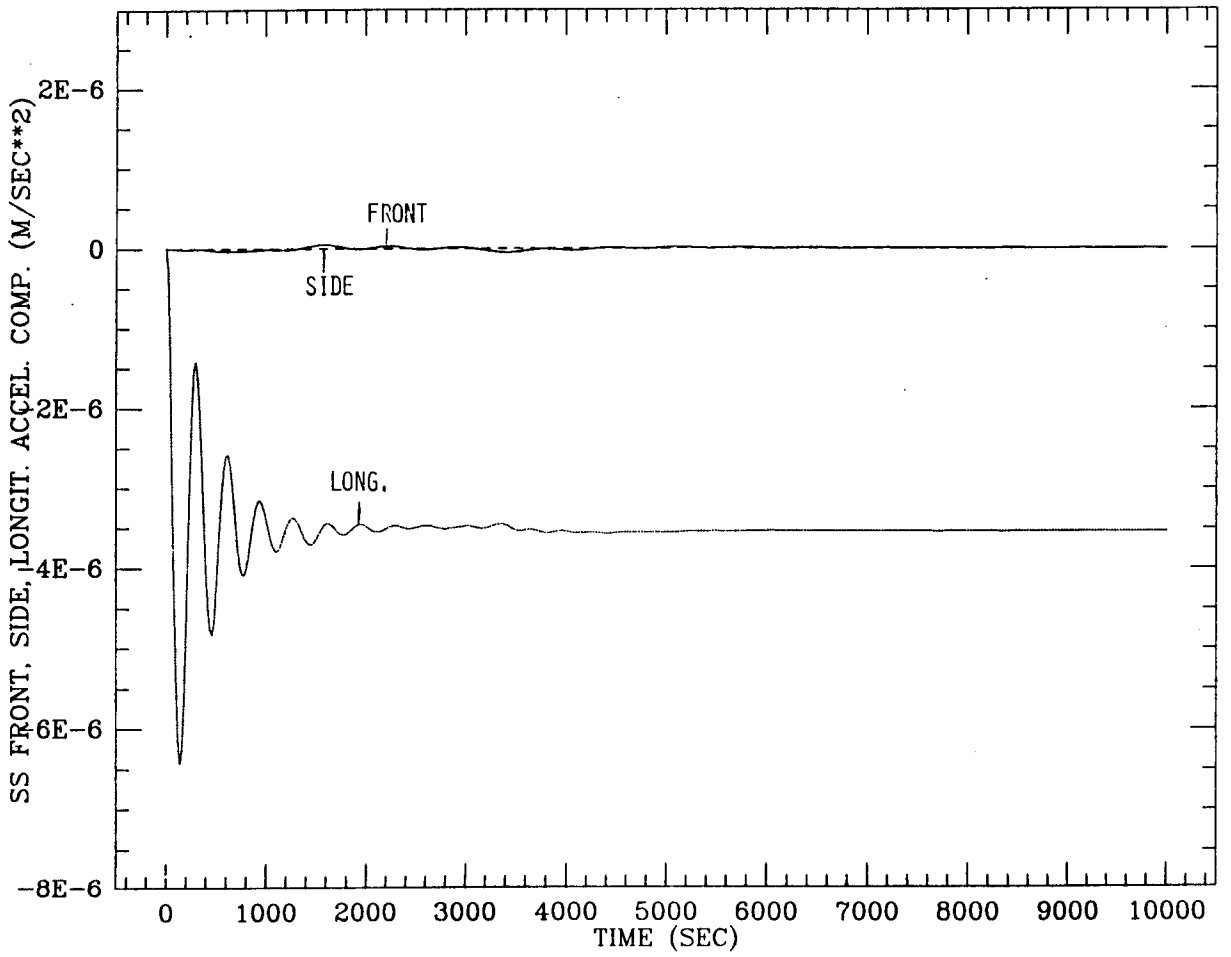
SS FRONT, SIDE, LONGIT. ACCEL. COMP. (M/SEC**2)
2E-6
0
-2E-6
-4E-6
-6E-6
-8E-6
FRONT
SIDE
LONG.
0
1000
2000
3000
4000
5000
6000
7000
8000
9000
10000
TIME (SEC)

Figure 2j.

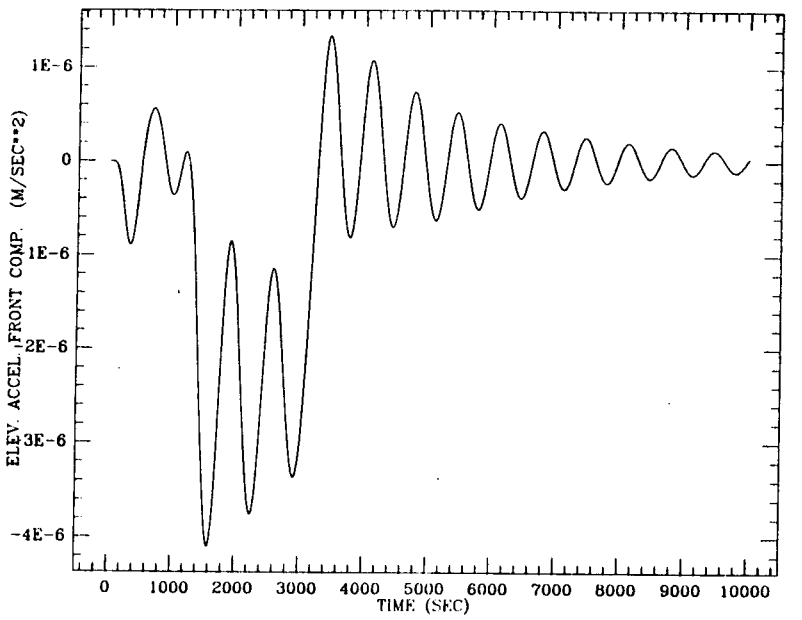

Figure 2k

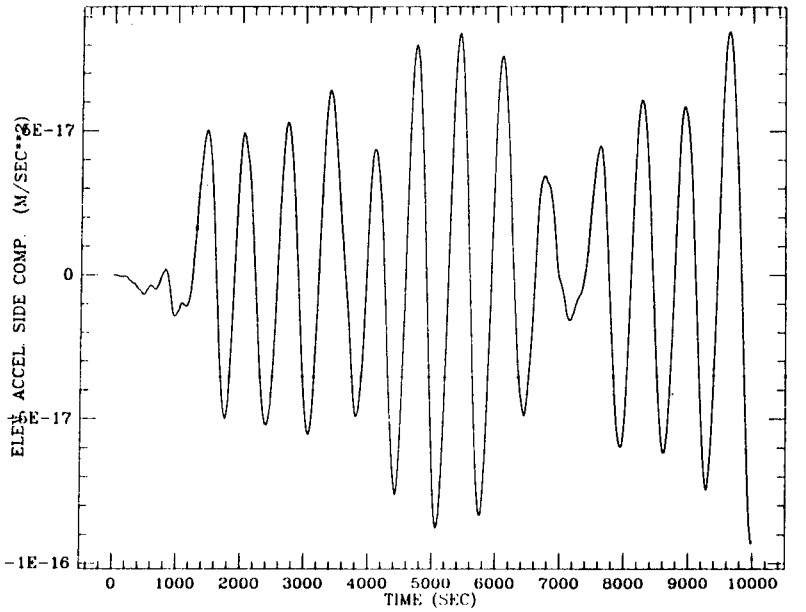

Figure 2ℓ

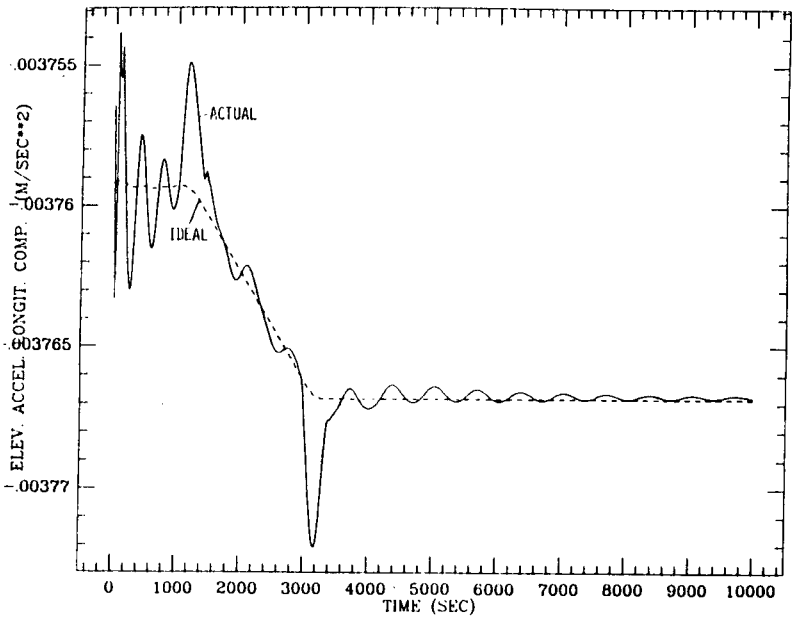

Figure 2m

difference between the final actual distance and the final controlled distance from the space station. Normally the final actual distance should be greater than the final controlled distance. In our case, however, the tension in tether 2, at the beginning of the elevator's maneuver, is greater than the steady state value. Consequently tether 2 is overstretched at the beginning of the maneuver explaining the slight negative difference at the end of the maneuver.

In simulation IIa all the environmental perturbations are acting upon the system. The total travelled length is 9.75 m instead of the 2 m of the previous case. The dynamic response is shown in Figures 3a through 3q. Figures 3a-3m are in the same sequence of the previous sets of figures. From inspection of Figure 3m it appears that the total variation of the ideal acceleration is comparable to the amplitude of the acceleration noise under steady state conditions (produced primarily by J_2 and by thermal shocks).

Figure 3n shows the temperature profile of tether 2 vs. time. This temperature profile is also applicable to simulation Ia. The thermal characteristics of kevlar tether are those indicated in Quarterly Report #6. Such characteristics are as follows: $\alpha = 0.4$, $\alpha_{IR} = 0.045$, $\epsilon = 0.9$, $c = 0.2$ Cal/Kg/°K. The temperatures of tether 1 and 3 are very close to that of tether 2 because the view factor of the three tether segments is almost the same. Figure 3p and 3q show the thermal stretch and the elastic stretch of tether 2. The initial temperature of the tether is assumed equal to 290 °K. Since kevlar has a negative thermal expansion coefficient the tether lengthens as it cools down.

Simulation IIa has also been rerun with environmental perturbations to generate simulation IIb. The results of simulation IIb are shown in Figures 4a through 4m. Figure 4m clearly shows the peaks of the maximum acceleration

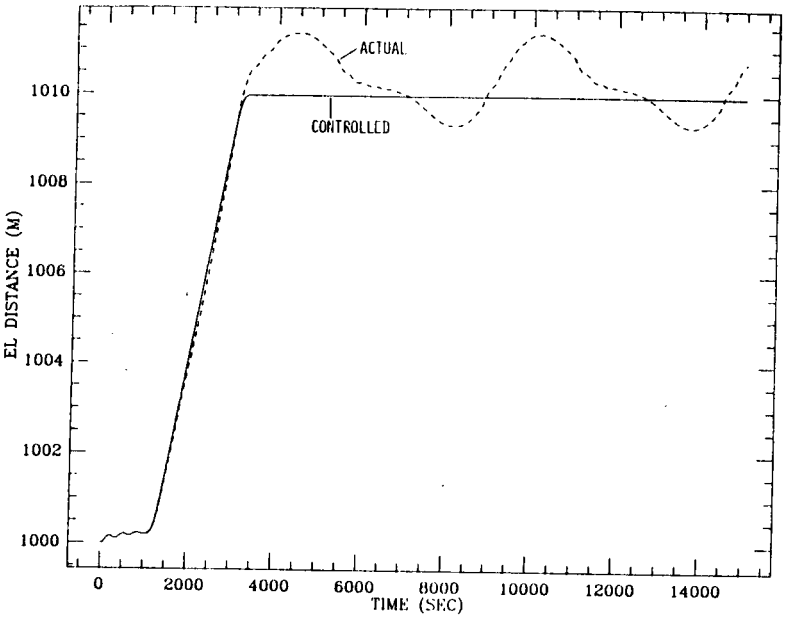

Figure 3a

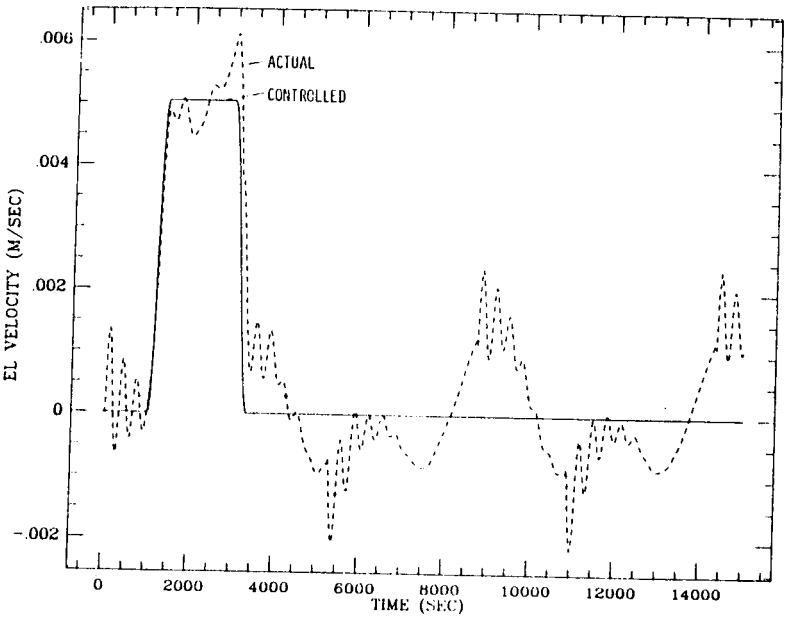

Figure 3b

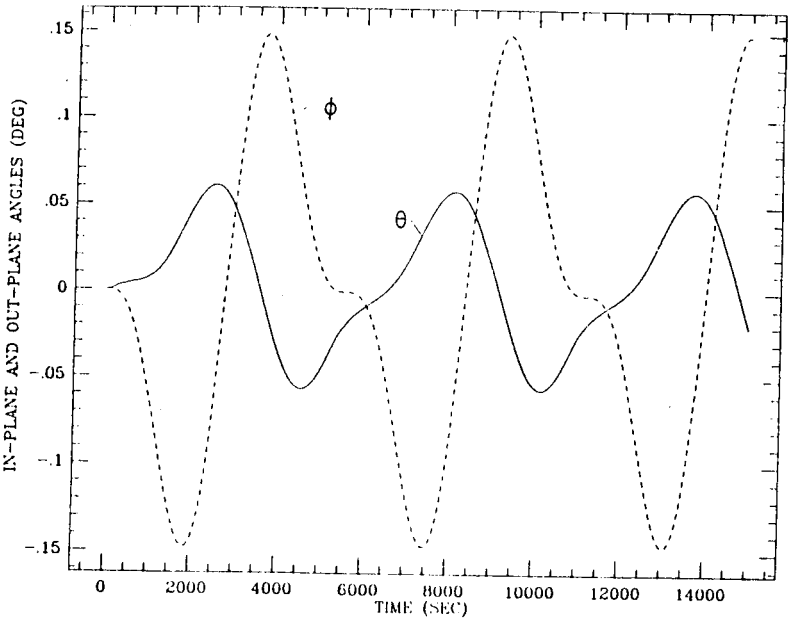

Figure 3c

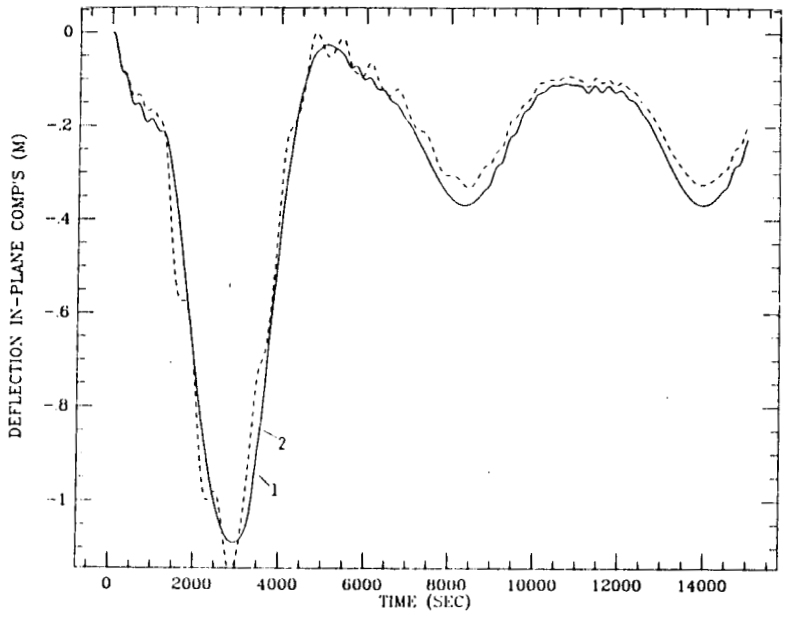

Figure 3d

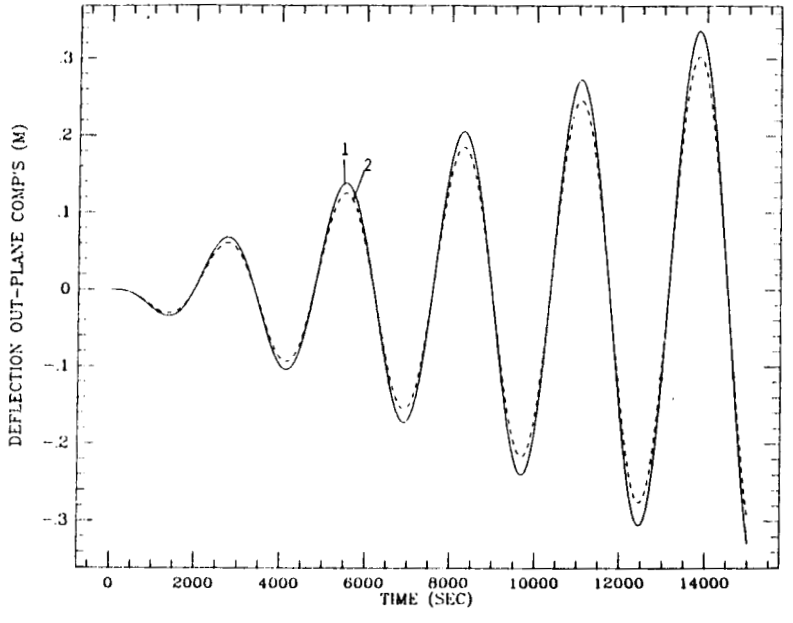

Figure 3e

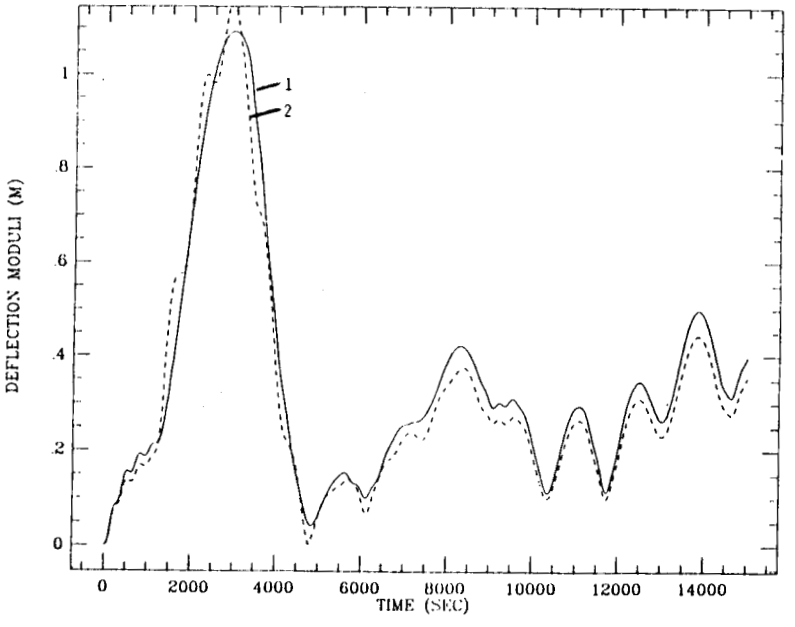

Figure 3f

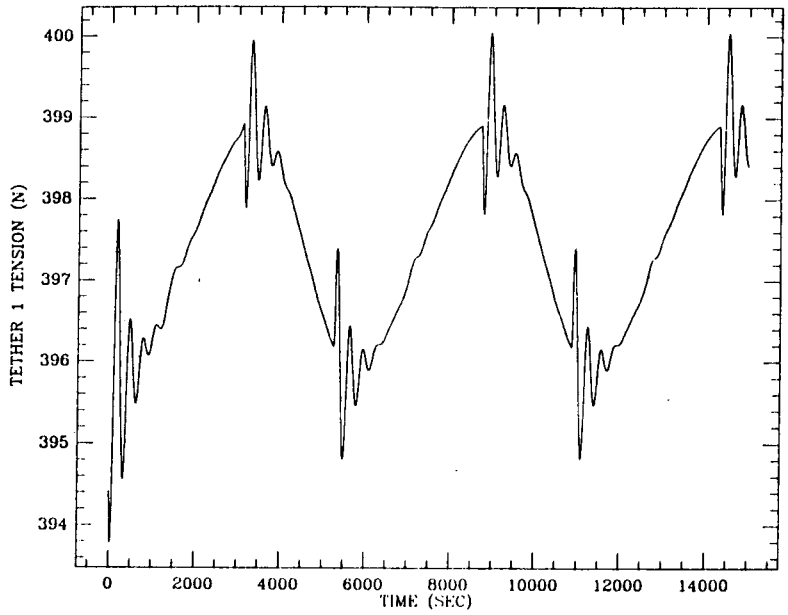

Figure 3g

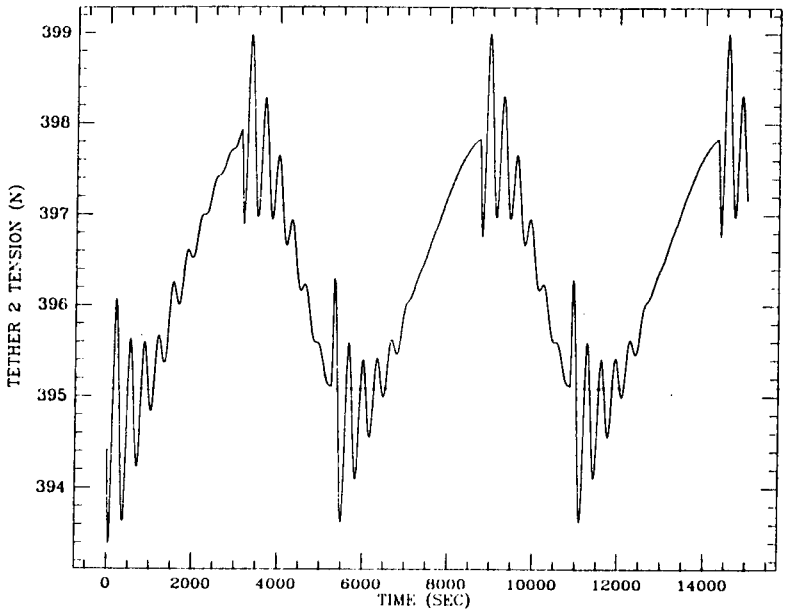

Figure 3h

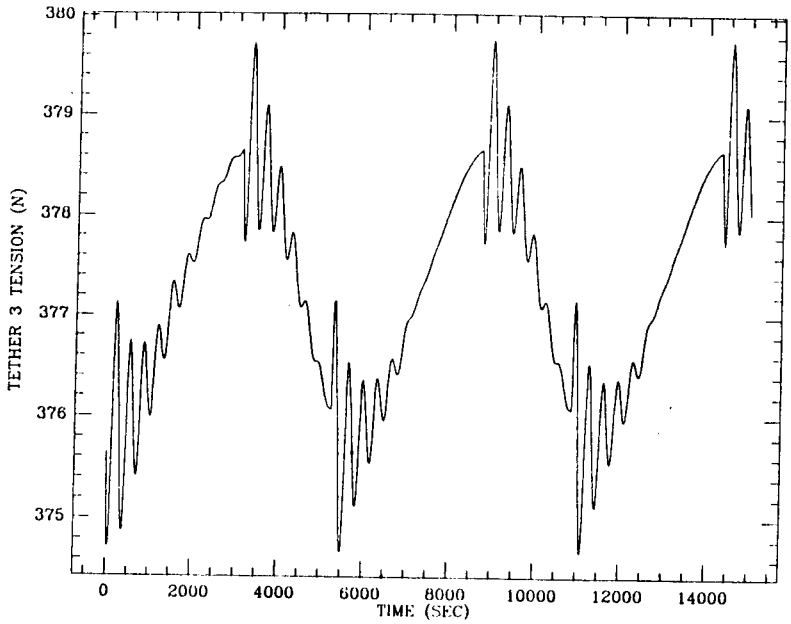

Figure 3i

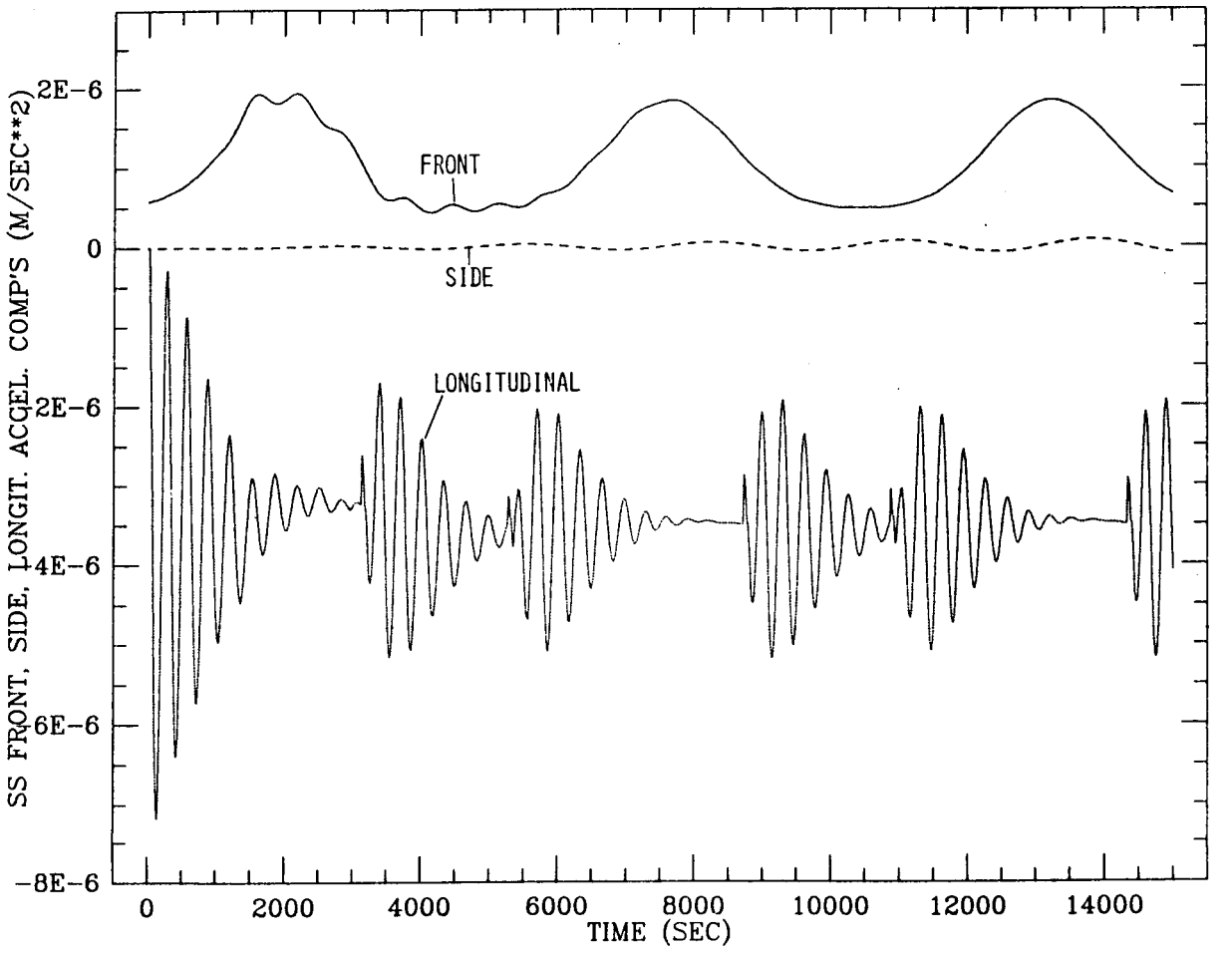
2E-6
0
-2E-6
-4E-6
-6E-6
-8E-6
SS FRONT, SIDE, LONGIT. ACCEL. COMP'S (M/SEC**2)
FRONT
SIDE
LONGITUDINAL
0
2000
4000
6000
8000
10000
12000
14000
TIME (SEC)

Figure 3j.

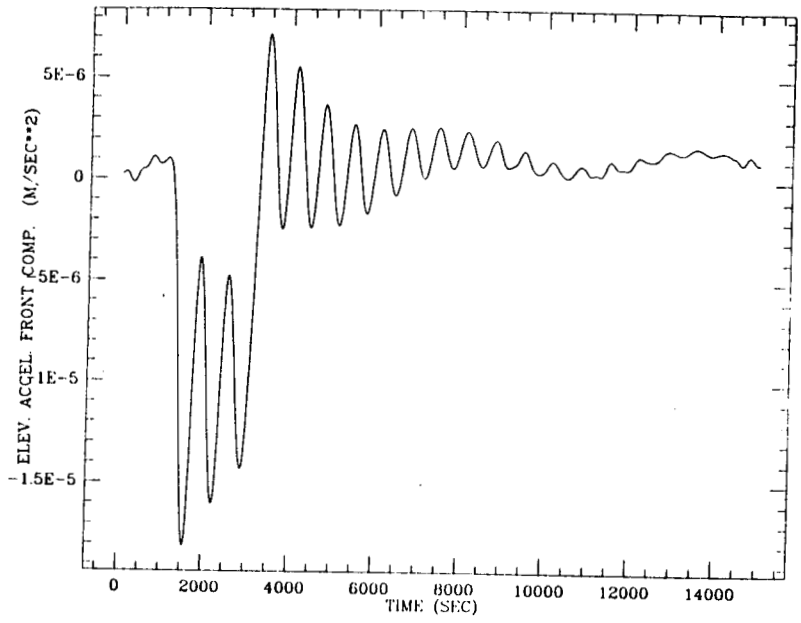

Figure 3k

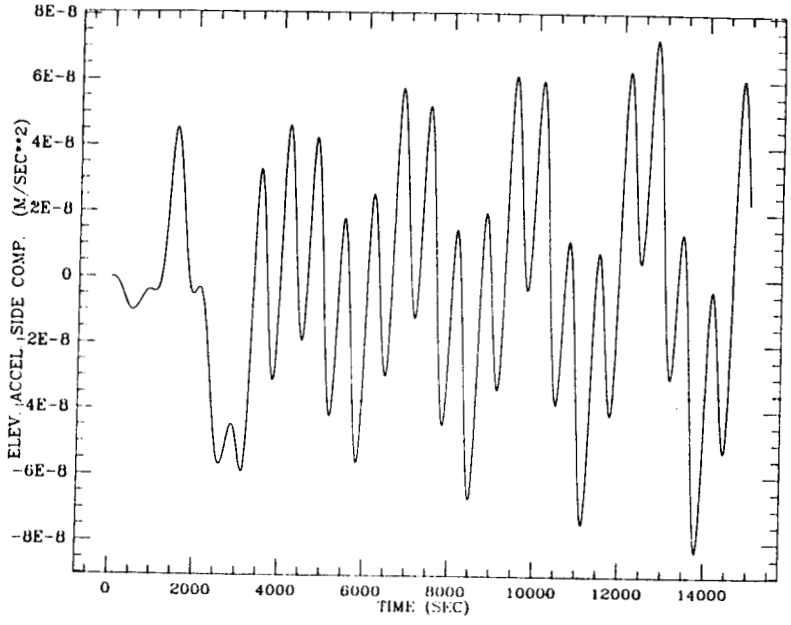

Figure 3ℓ

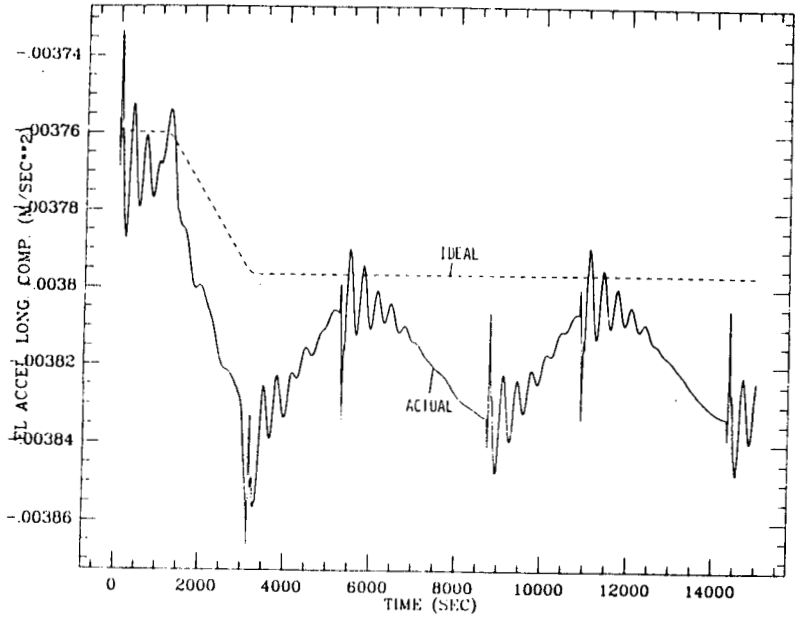

Figure 3m

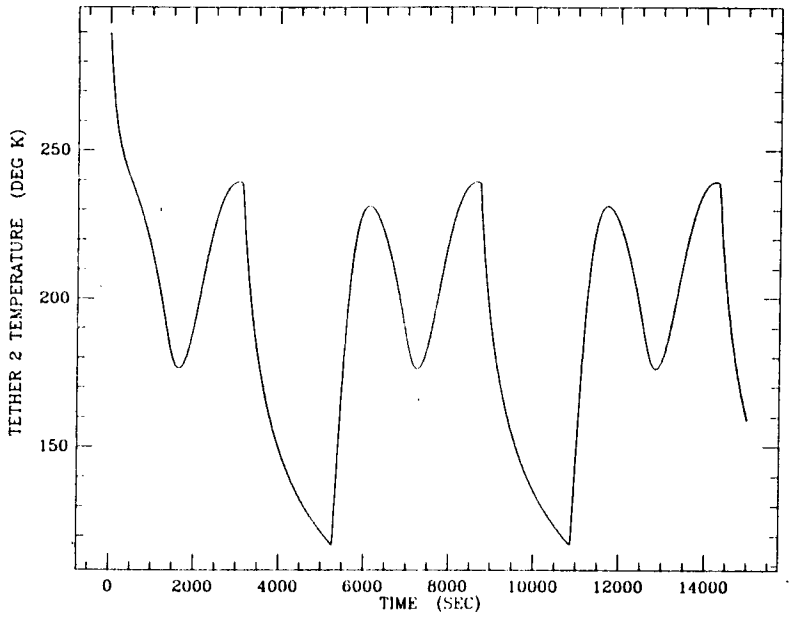

Figure 3n

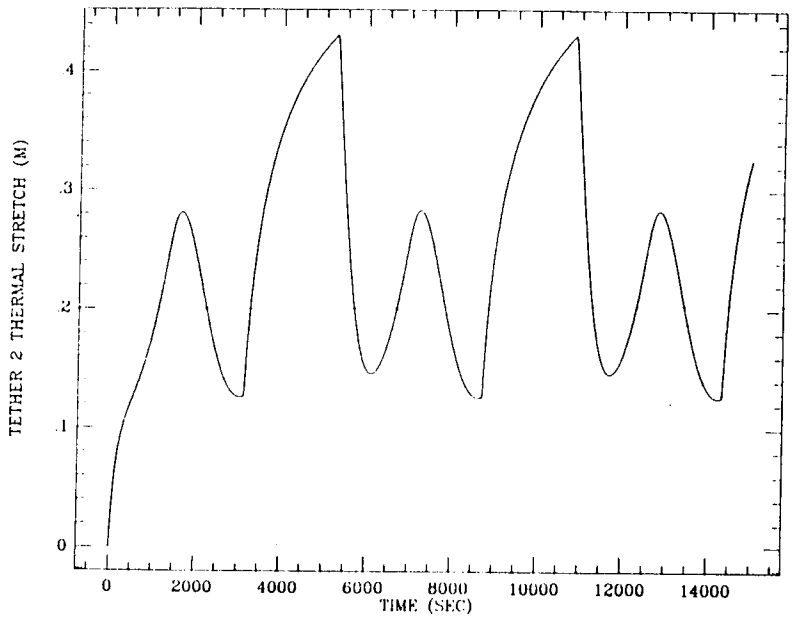

Figure 3p

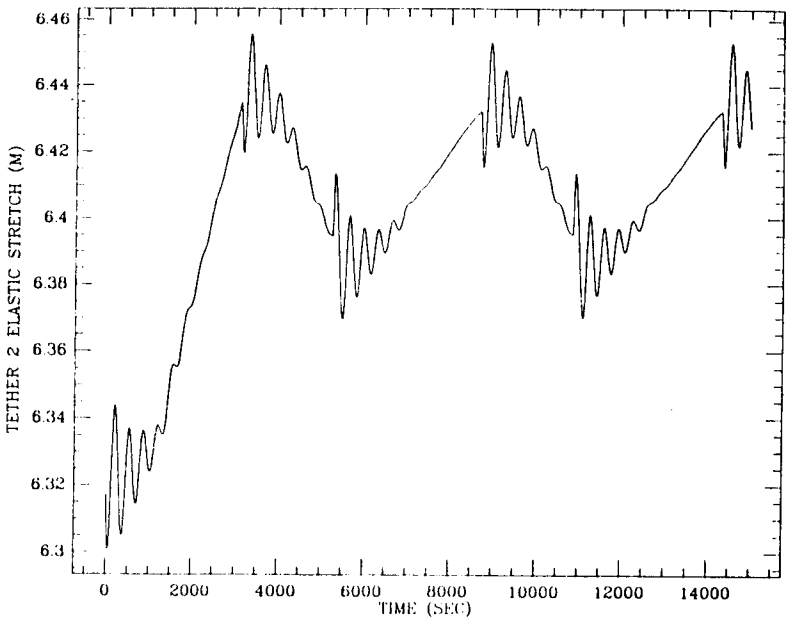

Figure 3q

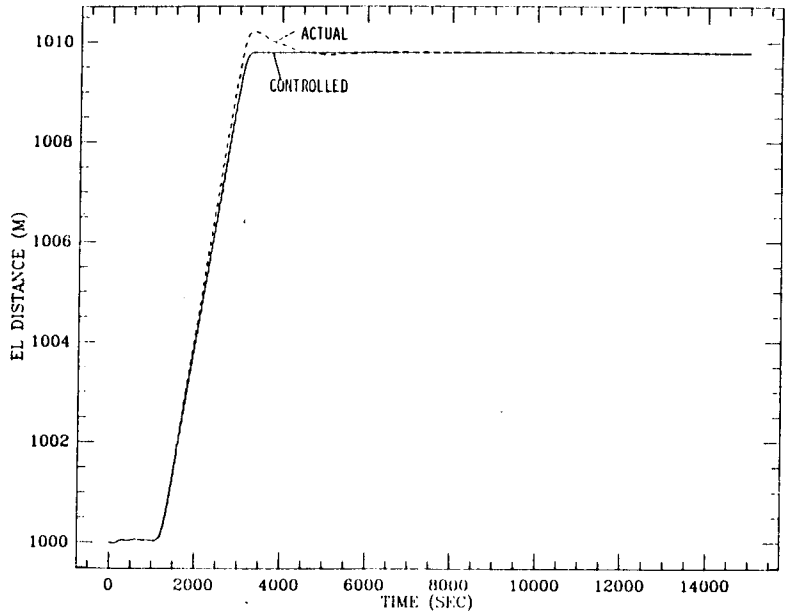

Figure 4a

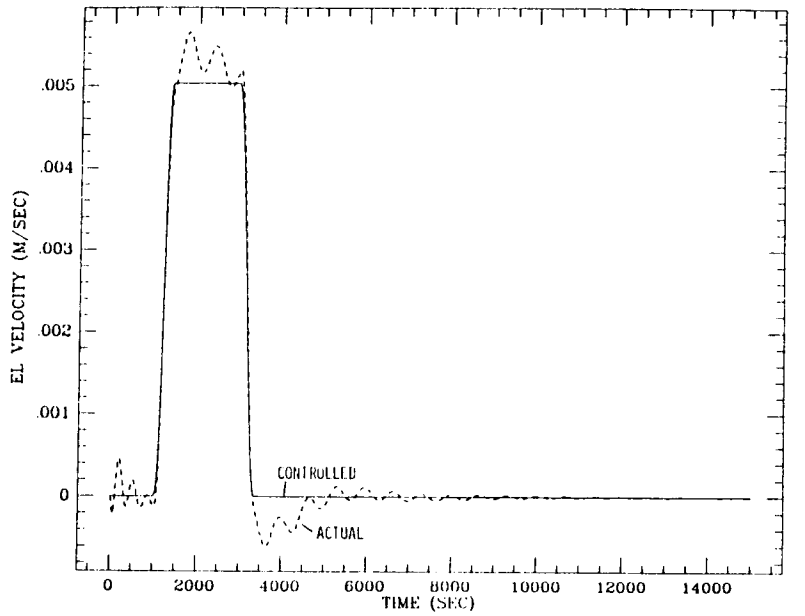

Figure 4b

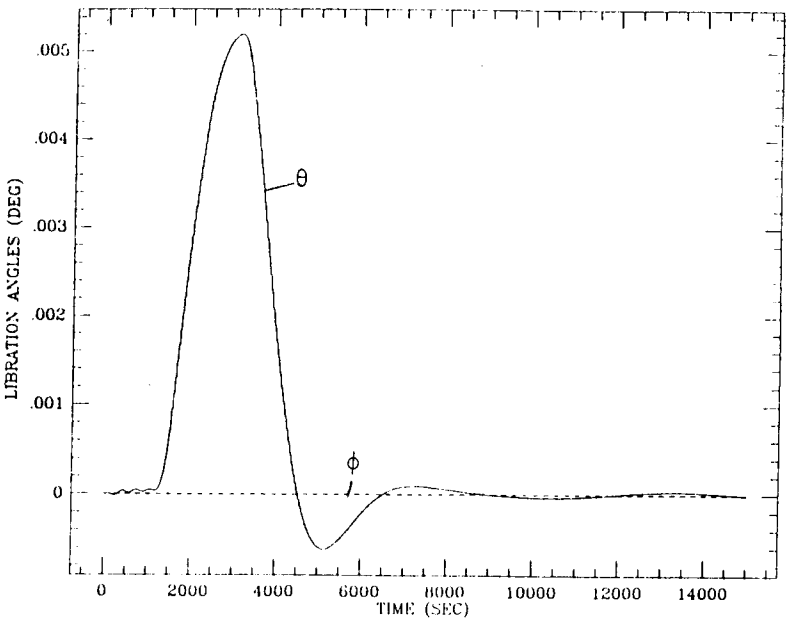

Figure 4c

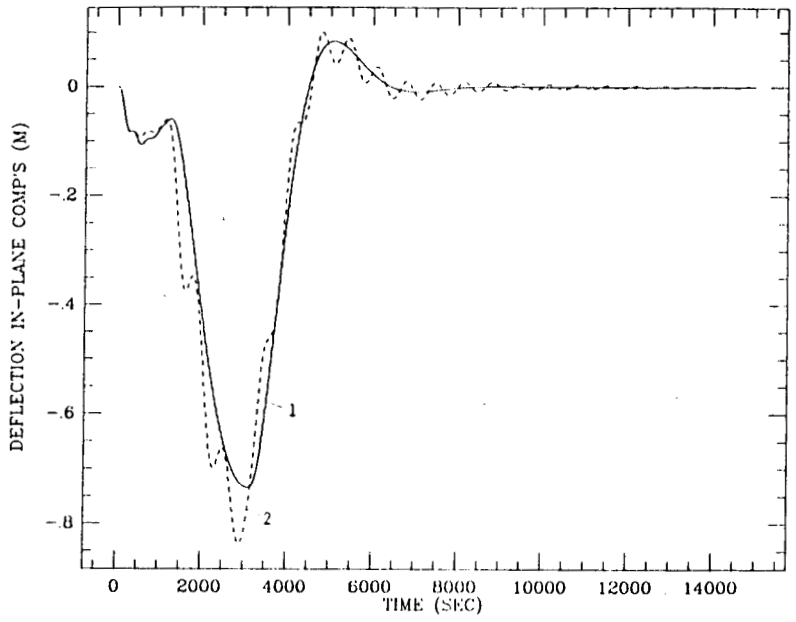

Figure 4d

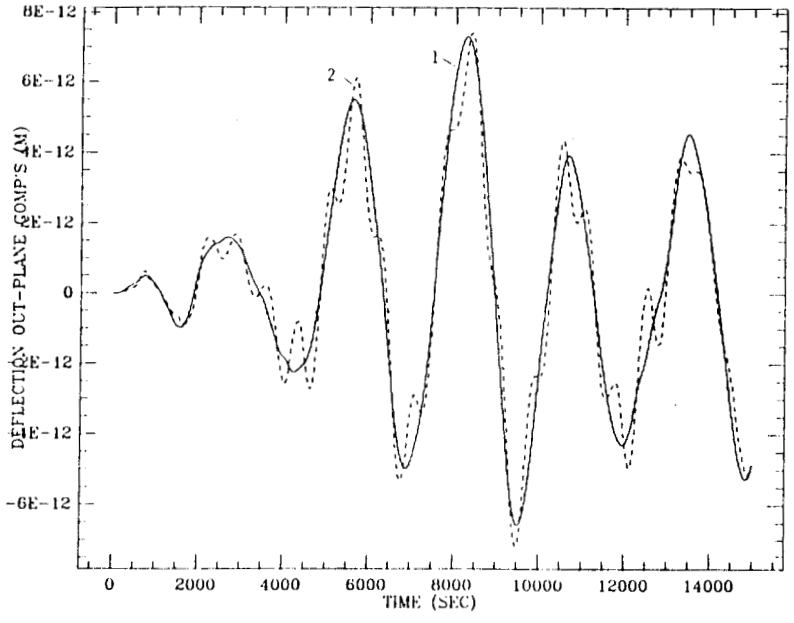

Figure 4e

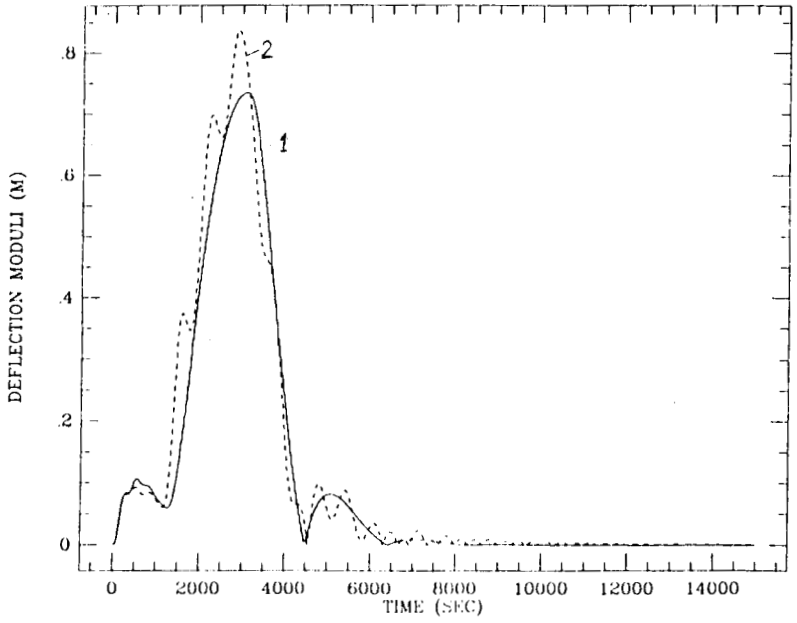

Figure 4f

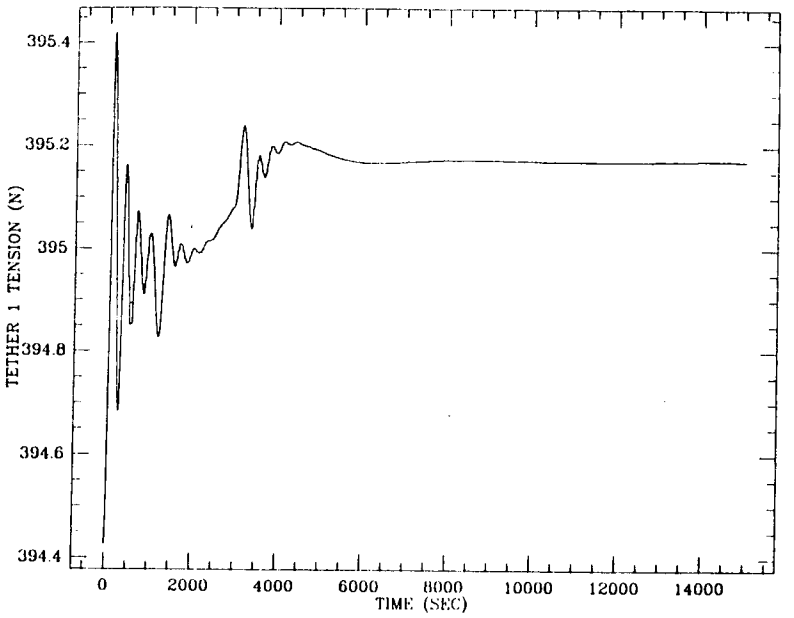

Figure 4g

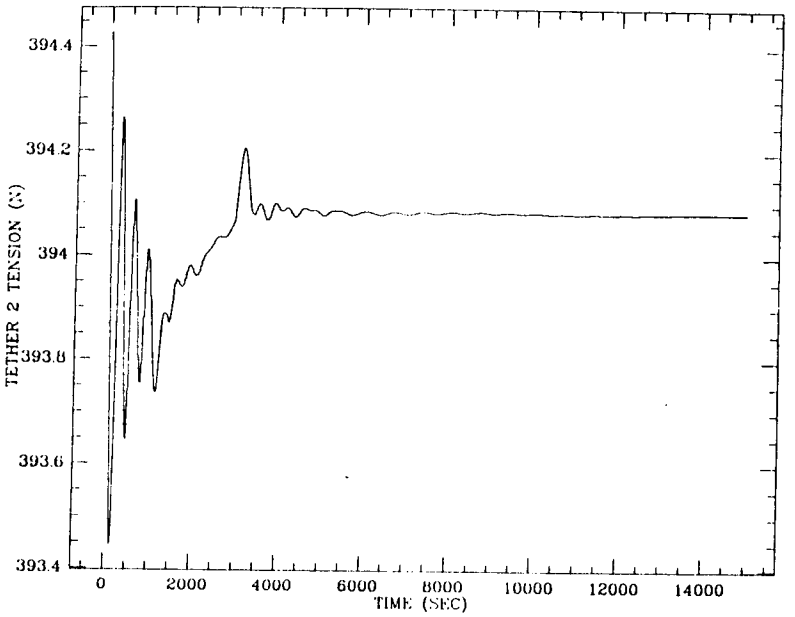

Figure 4h

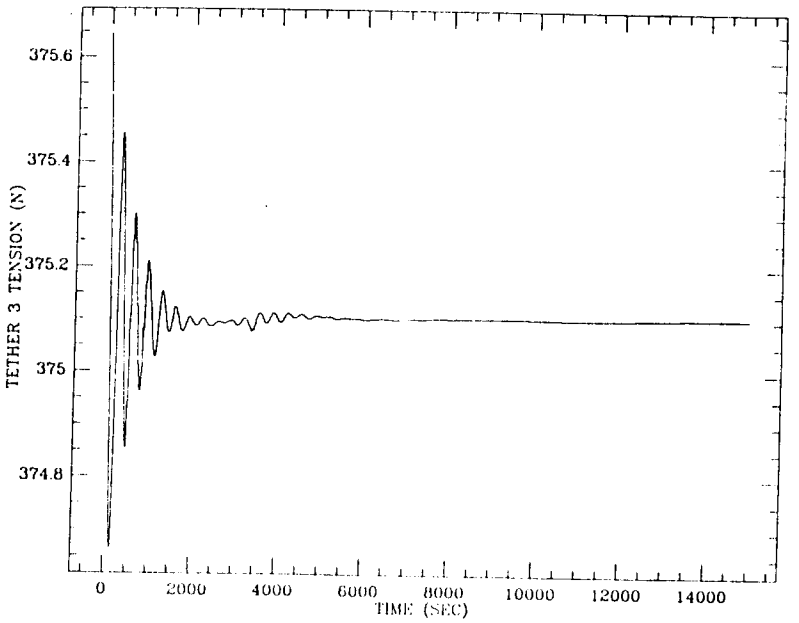

Figure 4i

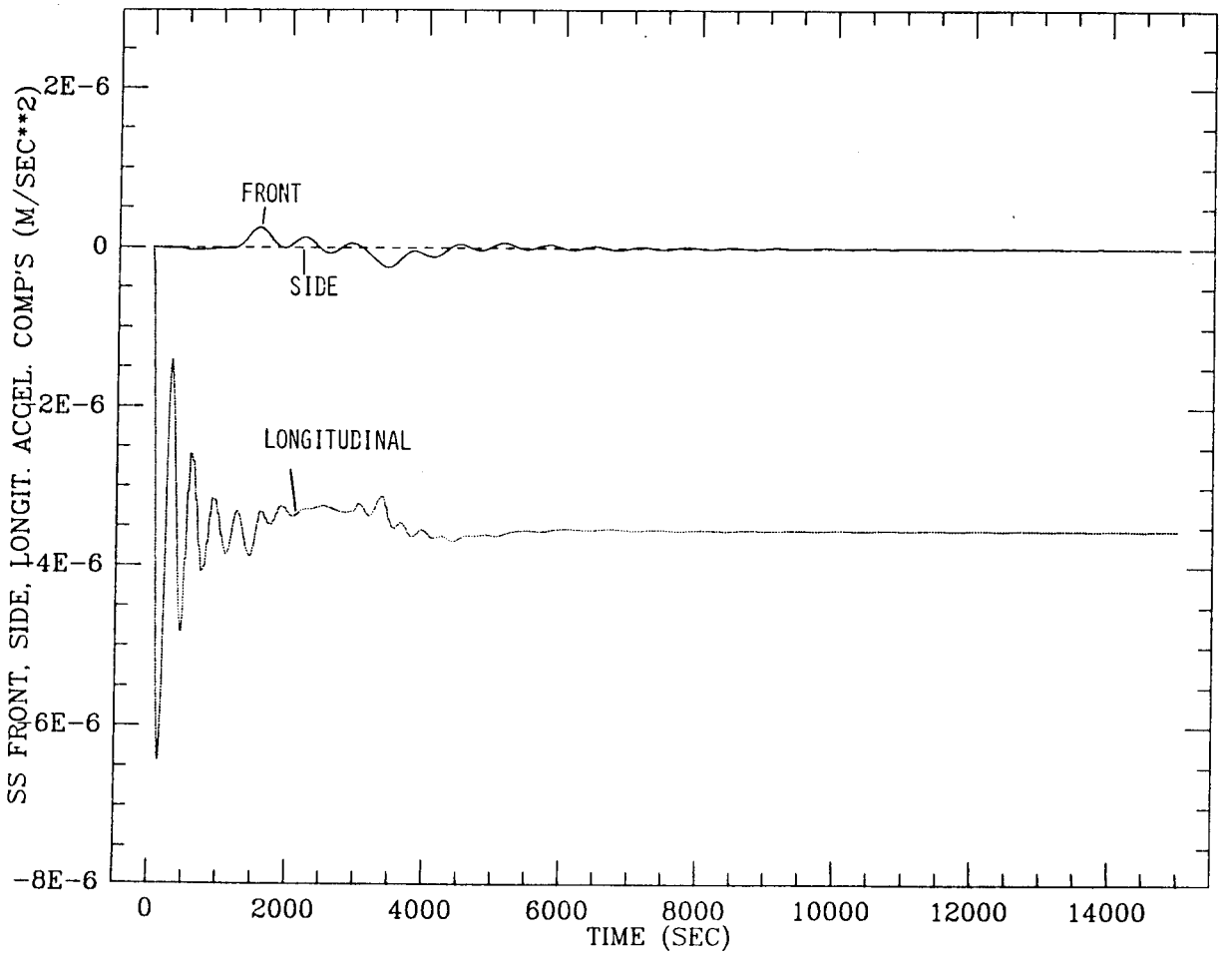
SS FRONT, SIDE, LONGIT. ACCEL. COMP'S (M/SEC**2)
2E-6
0
-2E-6
-4E-6
-6E-6
-8E-6
FRONT
SIDE
LONGITUDINAL
0
2000
4000
6000
8000
10000
12000
14000
TIME (SEC)

Figure 4j.

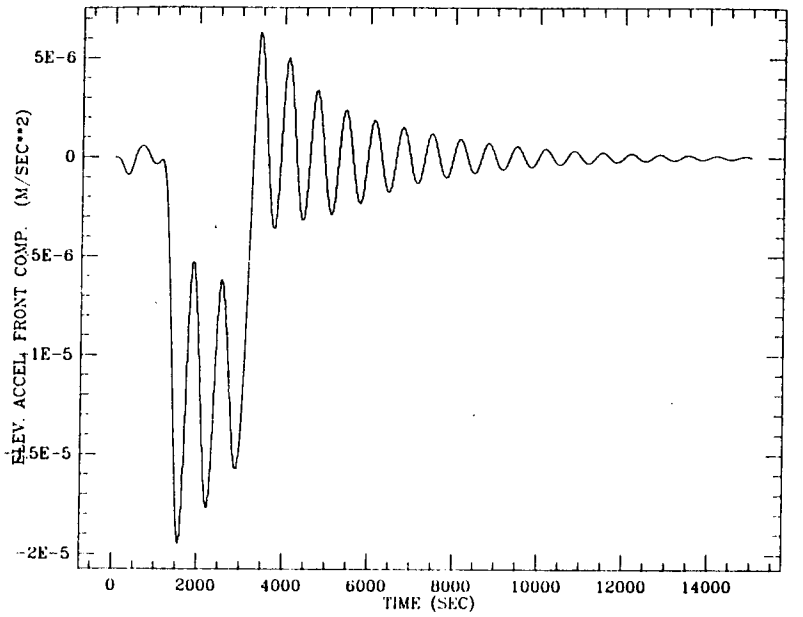

Figure 4k

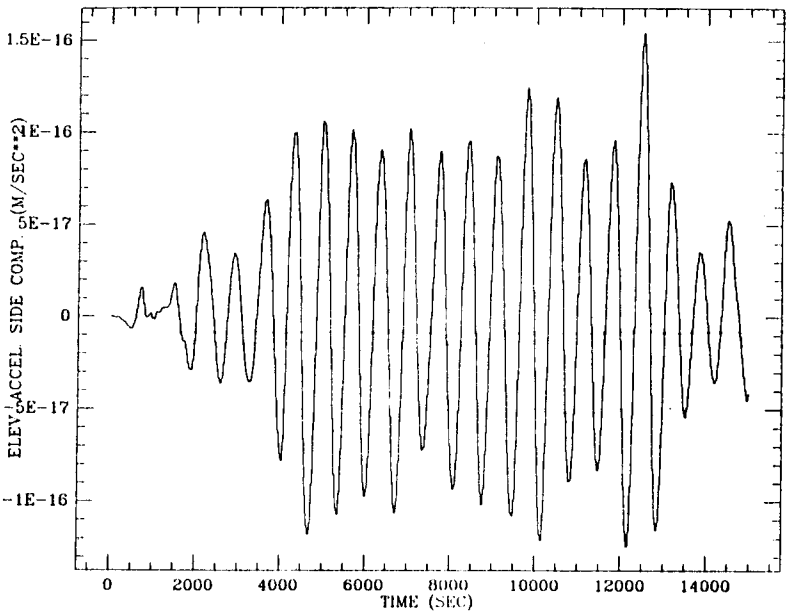

Figure 4ℓ

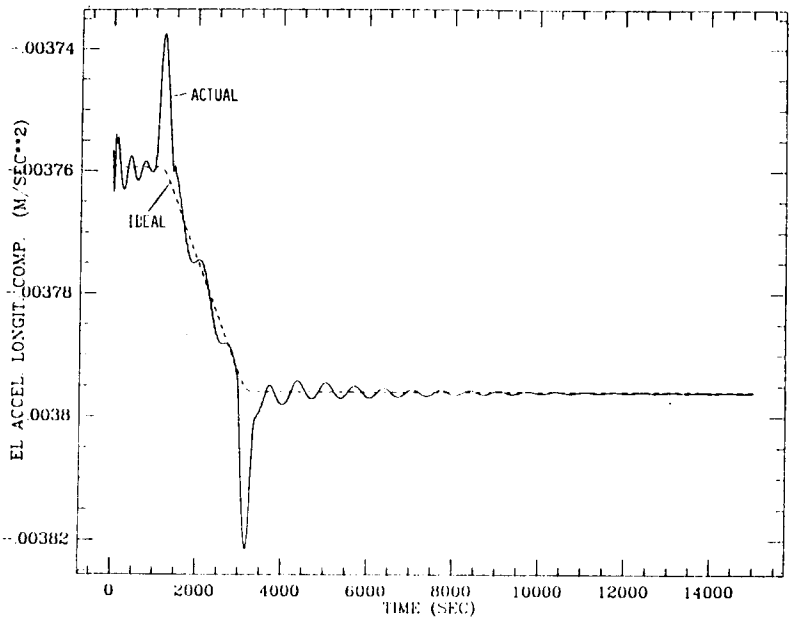

Figure 4m

and deceleration. It has already been noticed in the previous Quarterly Reports that these peaks are roughly proportional to α^2. The time constant $1/\alpha$ for all the previous simulations has been therefore set equal to 400 sec in order to reduce the magnitude of the acceleration peaks. These peaks do not meet the 10% criteria defined in Section 2.3 of Quarterly Report #8. The 10% criteria, however, is never met in the actual cases of the short distance maneuvers because of the noise level generated by the external perturbations. A more suitable criteria for short distance elevator's maneuvers in space is that the difference between the maximum acceleration produced by the elevator motion (i.e. the above mentioned peaks) and the ideal acceleration profile should be comparable to the amplitude of the acceleration noise produced by external perturbations. By adopting $1/\alpha \geq$ 400 sec this criteria is met.

2.1.2 Long Distance Crawling Maneuvers With Mirror Image Motion Control Law

The mirror image motion control law has been adopted to perform a long distance crawling maneuver. The travelled length and control parameters are like those adopted for the *MHTCL* of Quarterly Report #8. Such parameters are as follows:

$$\Delta \ell_{cT} = 4km, \ 1/\alpha = 1000 \text{ sec}, \ \gamma = 4, \ Y = 0.8 \tag{7}$$

Two simulation runs have been performed under the above mentioned conditions: 1) in simulation IIIa all the environmental perturbations are acting upon the system; 2) in simulation IIIb only the gravity perturbation J_2 is acting. Simulation IIIb has been done in order to compare the results obtained by adopting

the *MIMCL* with those obtained in Quarterly Report #8 by adopting the *MHTCL*.

The dynamic response of the system under the conditions of simulation IIIa are shown in Figures 5a through 5m. Unlike the case of the short distance maneuvers, the controlled distance of the elevator is corrected beforehand to take into account the tether elasticity (but not the thermal stretch) in order to have a final actual distance from the space station of 5 km. By comparing Figure 5b with Figure 2g of Quarterly Report #8 it can be immediately noticed that the *MIMCL* is 40% faster than the *MHTCL*. Referring to Figure 5m, the small difference between the ideal and the actual value of the *EL* longitudinal acceleration, after the maneuver, is owing to the thermal stretch (which has not been taken into account when we corrected the controlled distance) and to a smaller extent to the J_2-generated-tether-stretch.

The dynamic response under the conditions of simulation IIIb is shown in Figures 6a through 6m. By comparing this set of figures to the previous set we can conclude that, for long distance crawling maneuvers, the largest perturbations are produced by the J_2 gravity term. The libration angles and the lateral deflections of the inner-masses are the same for the two simulation runs. The acceleration levels on board the space station and the elevator are very similar for the two cases. Drag and thermal effects, therefore, can be neglected if we are interested in evaluating the acceleration time history during a long distance crawling maneuver. Such perturbations, however, should not be neglected when we explore the acceleration levels under steady state conditions.

We compare the results of simulation IIIb to those obtained by using the *MHTCL* in Quarterly Report #8 under the same control parameters. The results are quite similar. The lateral deflections are slightly higher for the *MIMCL* case.

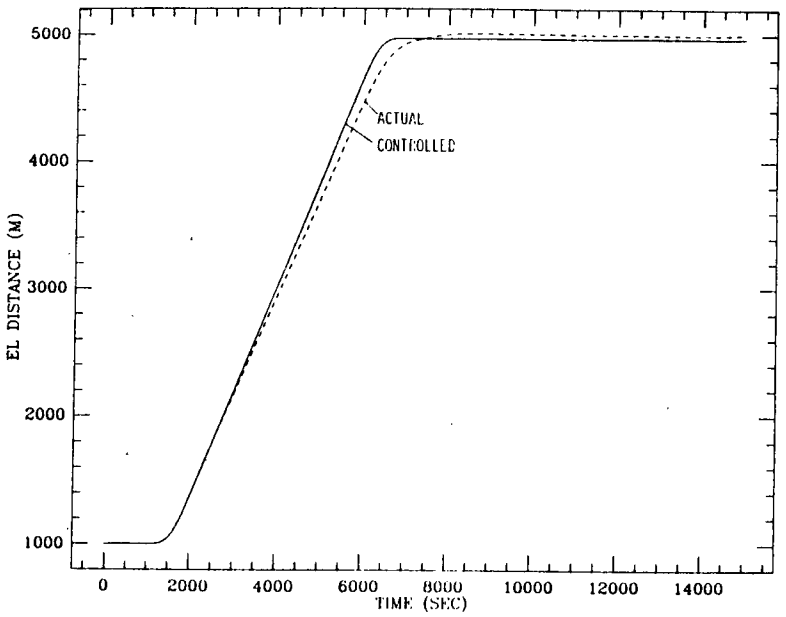

Figure 5a

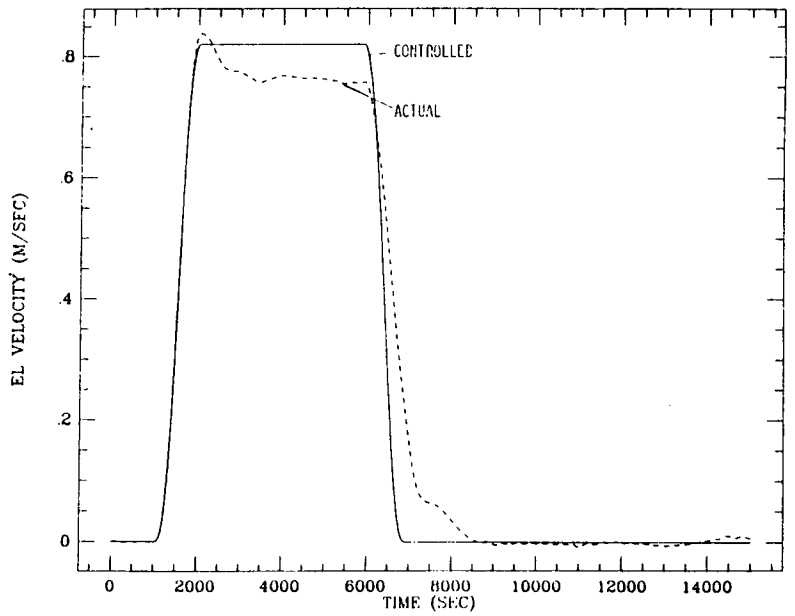

Figure 5b

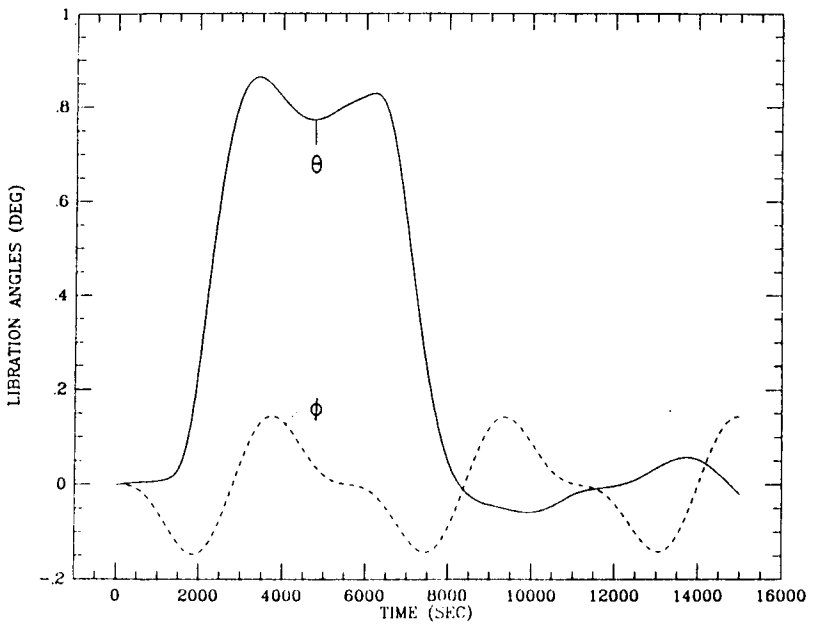

Figure 5c

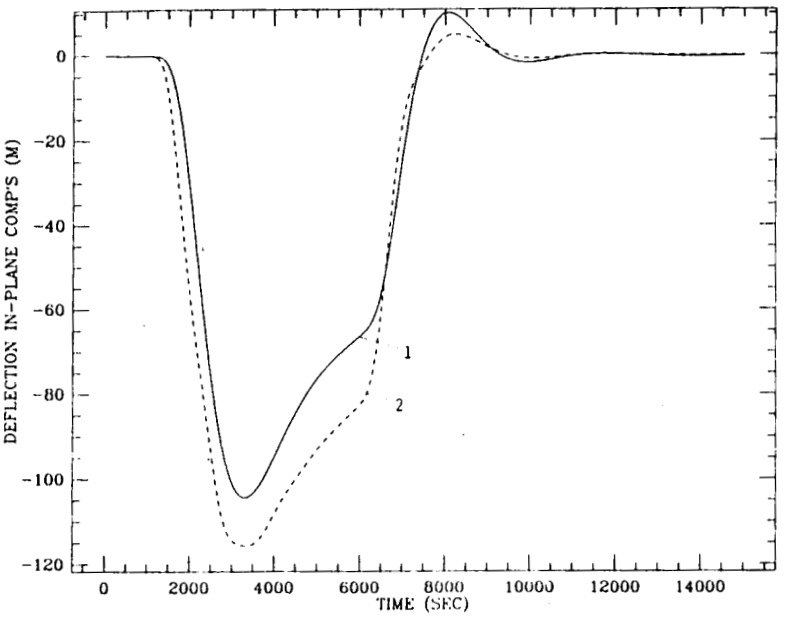

Figure 5d

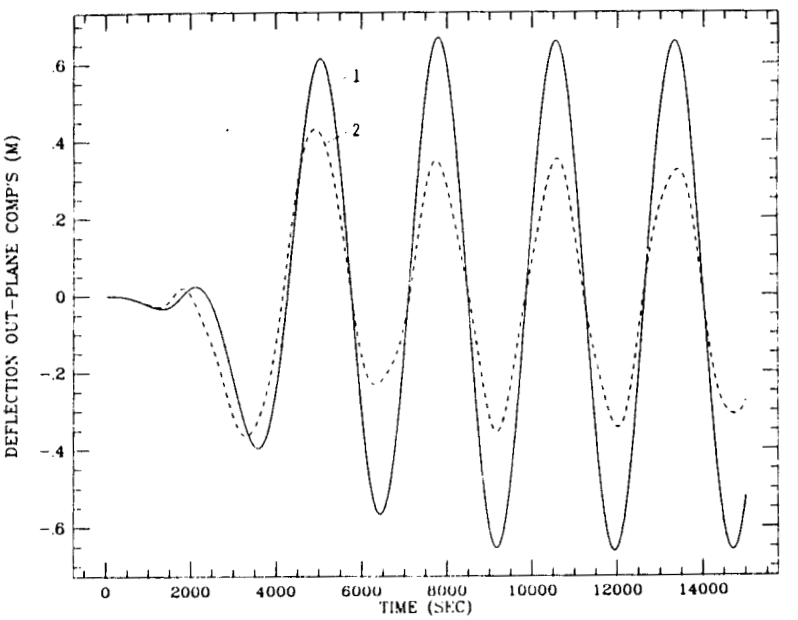

Figure 5e

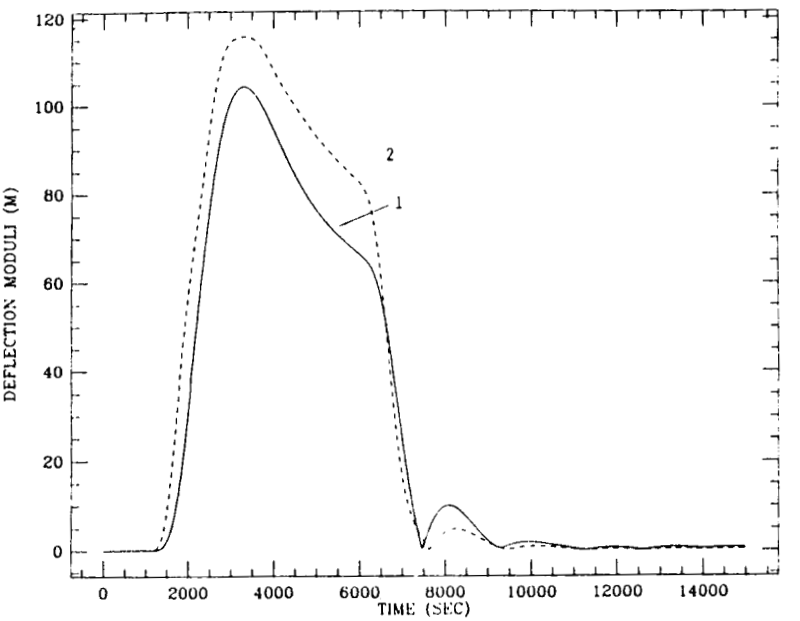

Figure 5f

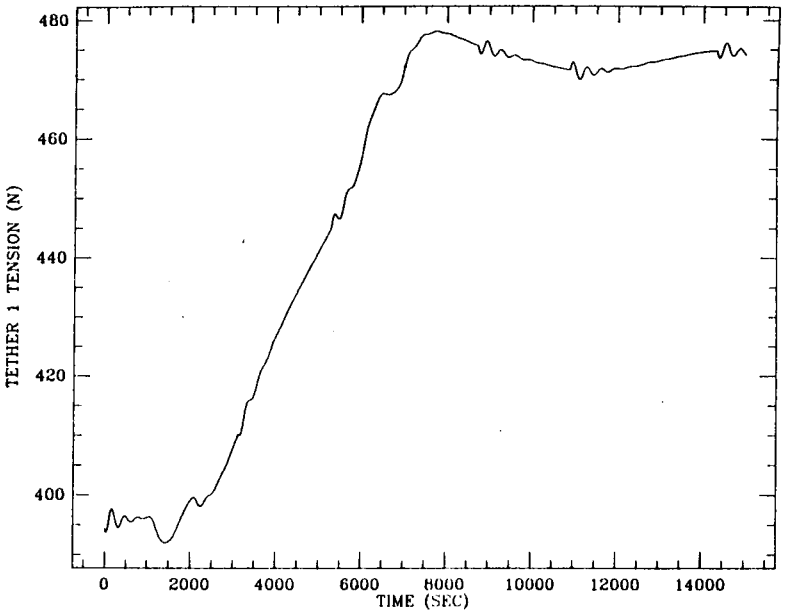

Figure 5g

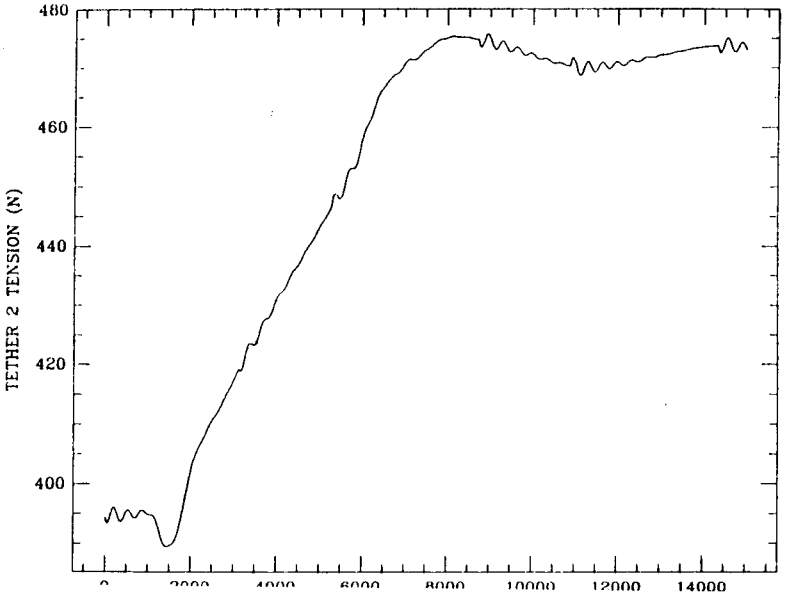

Figure 5h

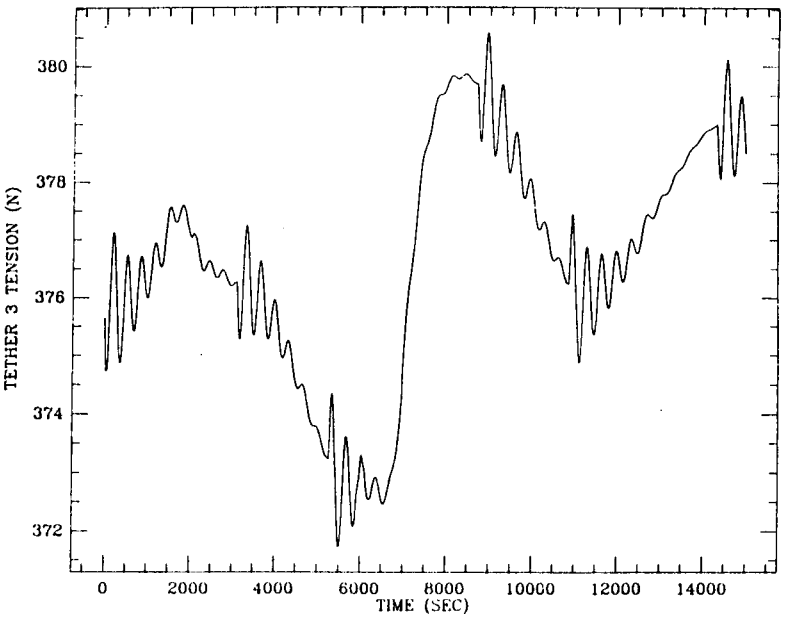

Figure 5i

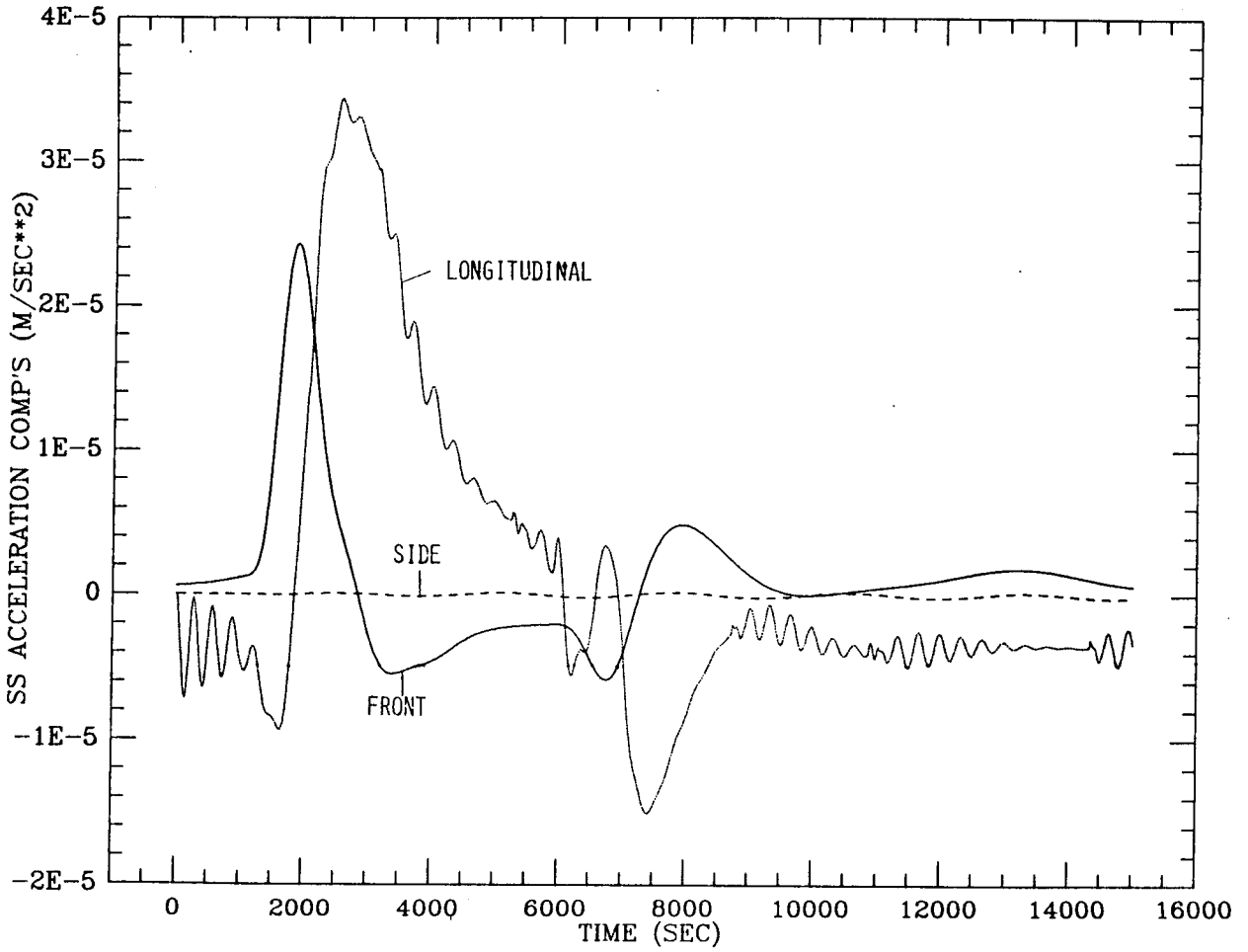
4E-5
3E-5
2E-5
1E-5
0
-1E-5
-2E-5
SS ACCELERATION COMP'S (M/SEC**2)
LONGITUDINAL
SIDE
FRONT
0
2000
4000
6000
8000
10000
12000
14000
16000
TIME (SEC)

Figure 5j.

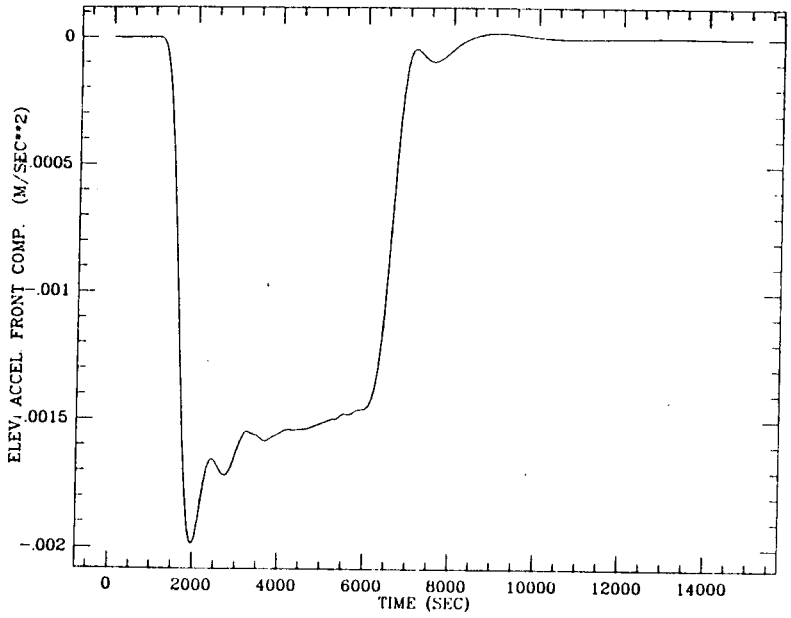

Figure 5k

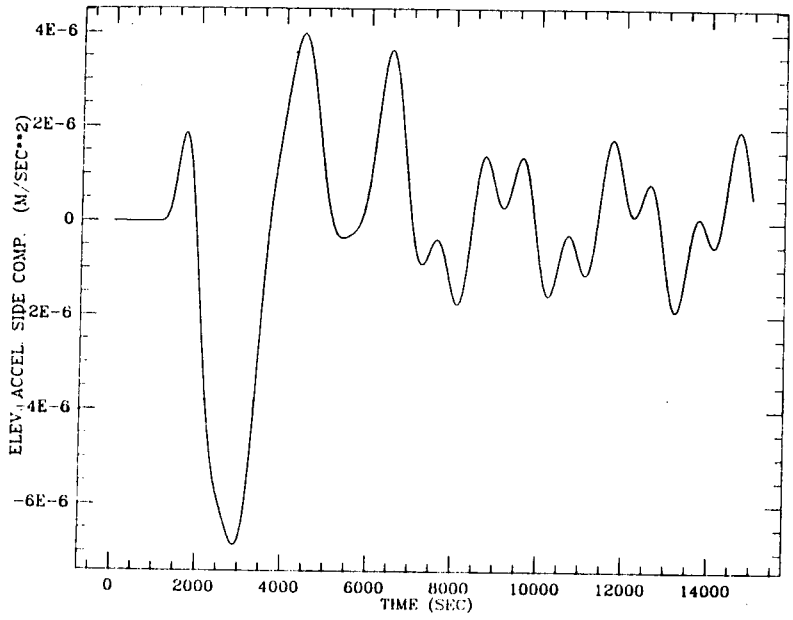

Figure 5ℓ

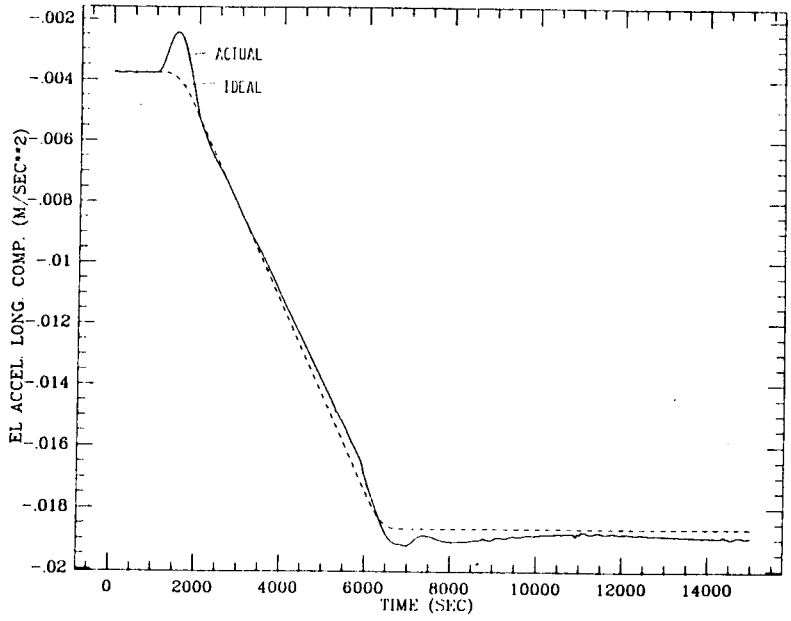

Figure 5m

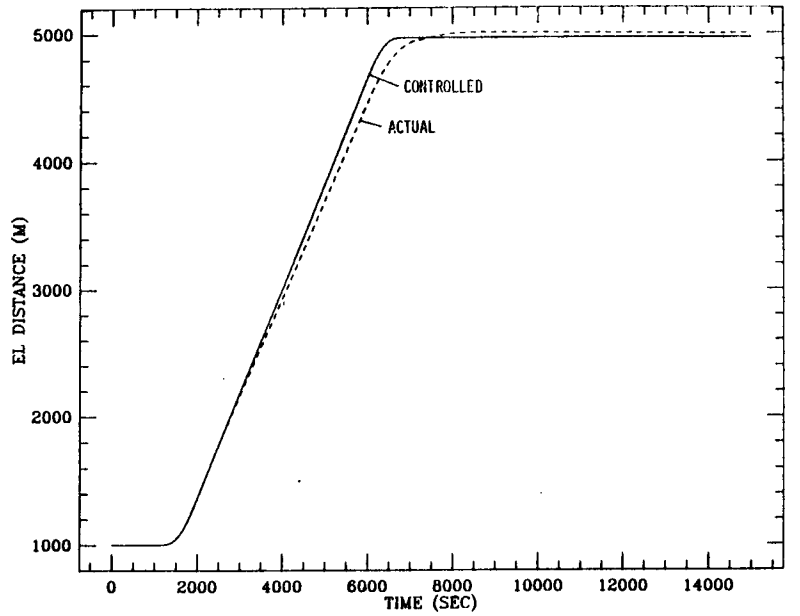

Figure 6a

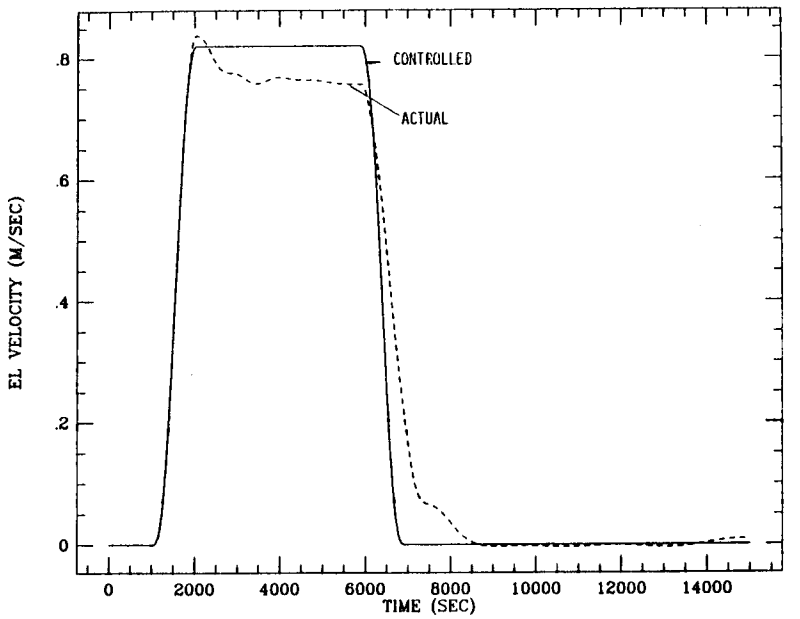

Figure 6b

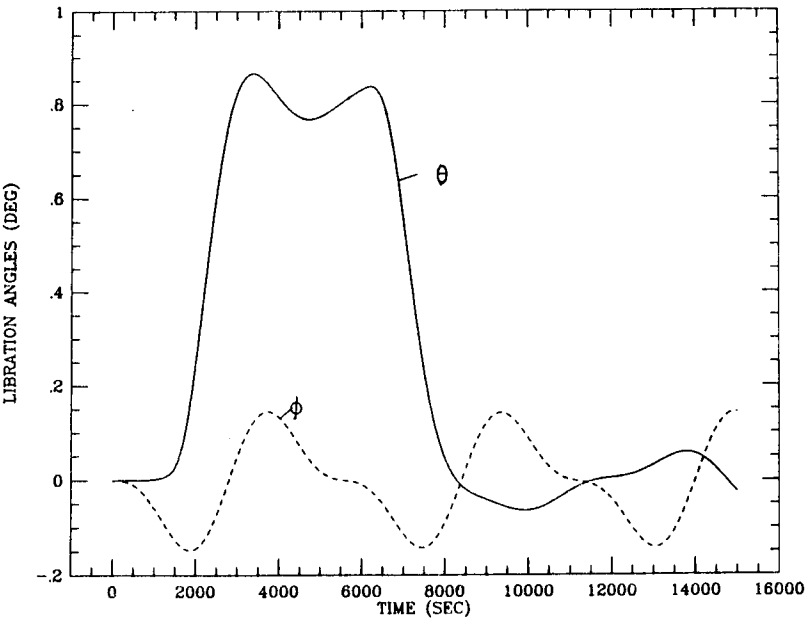

Figure 6c

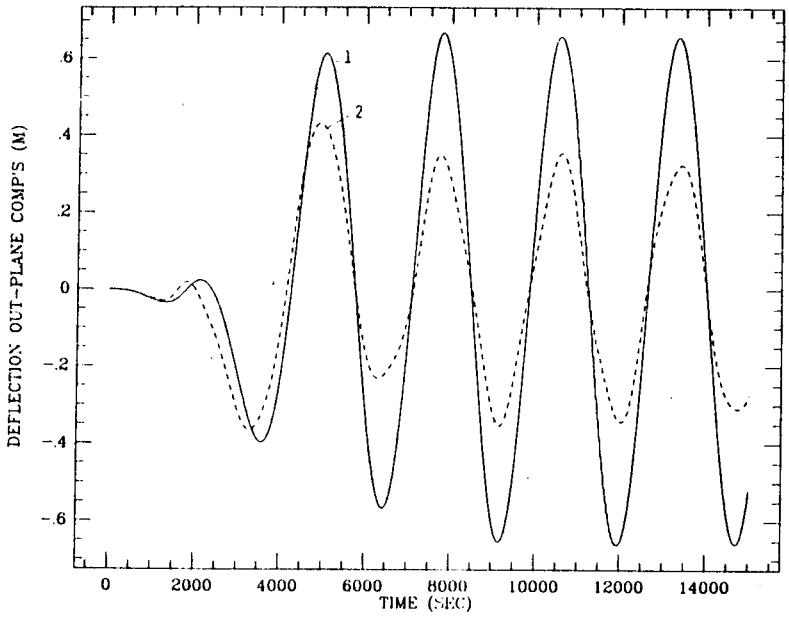

Figure 6d

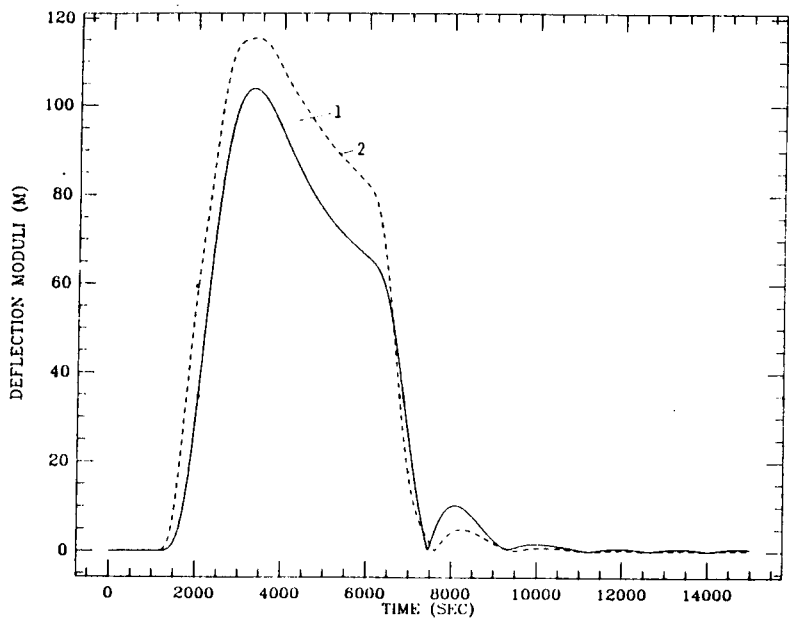

Figure 6e

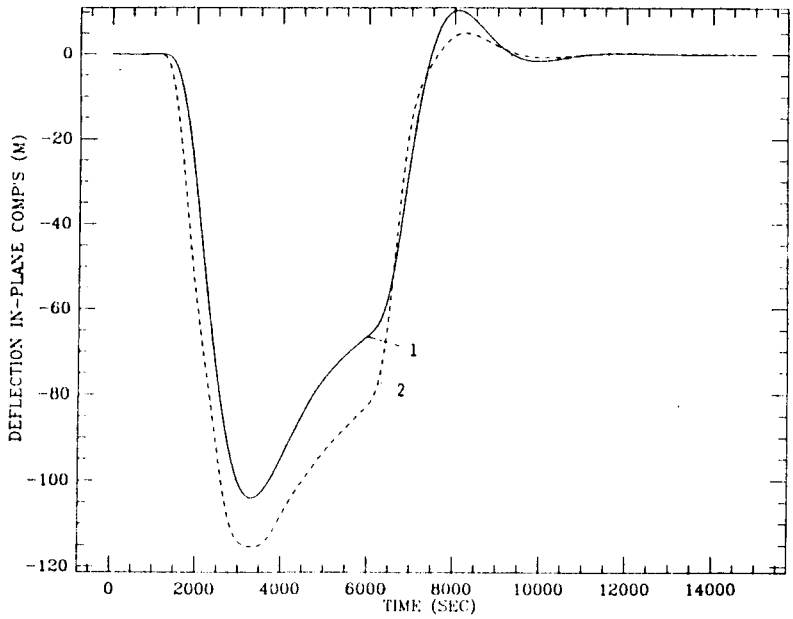

Figure 6f

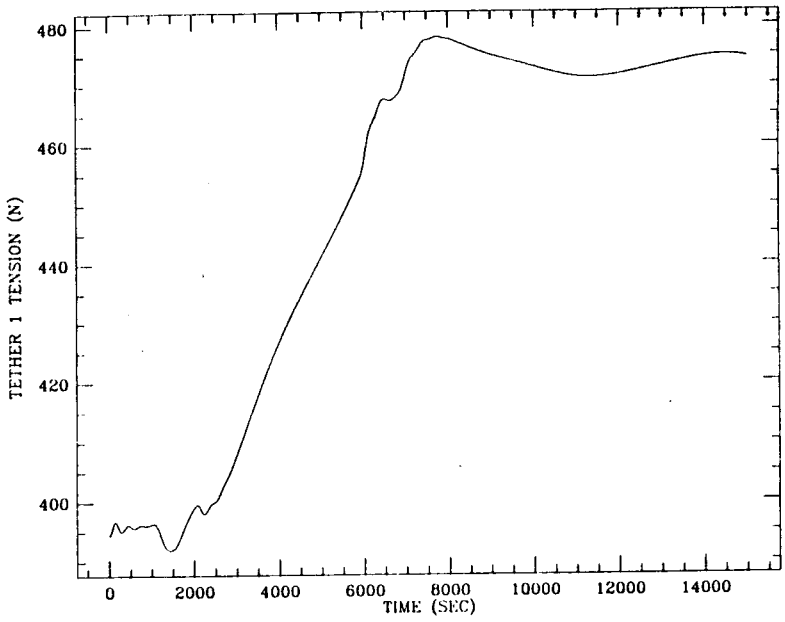

Figure 6g

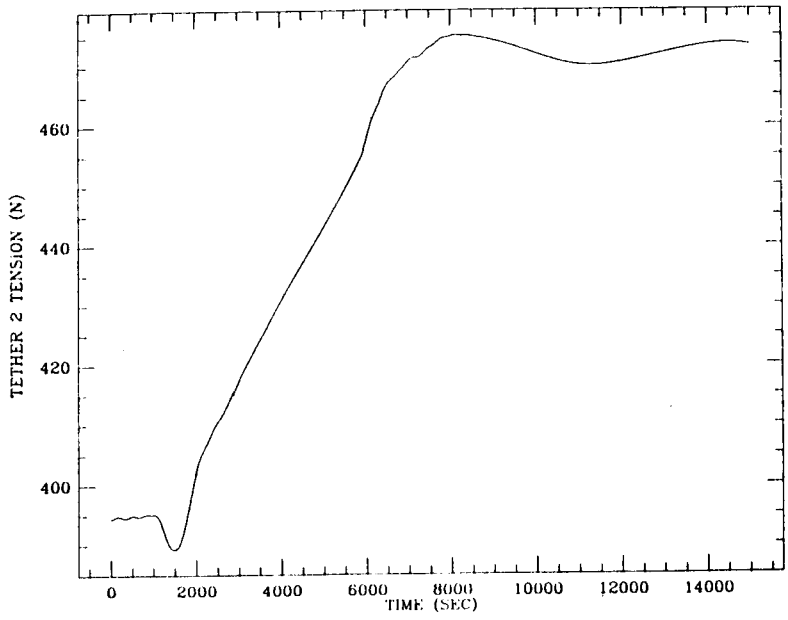

Figure 6h

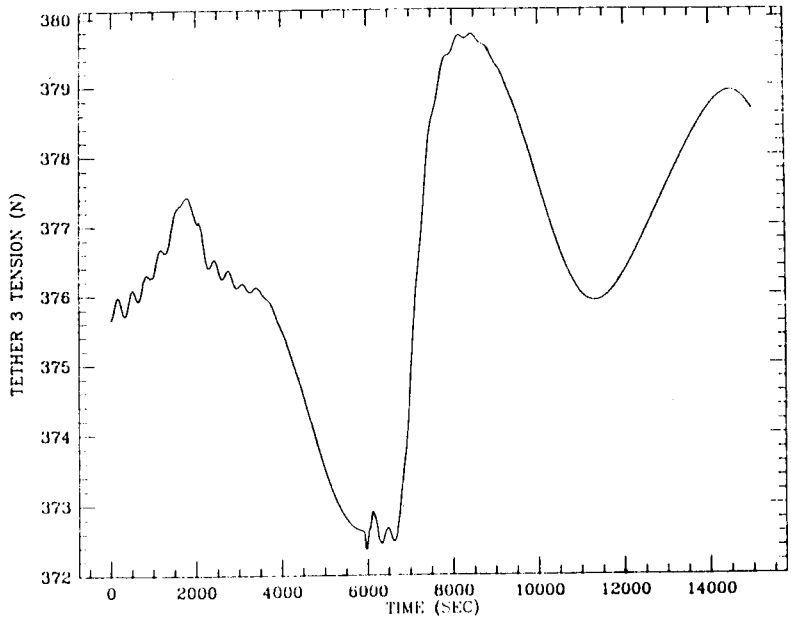

Figure 6i

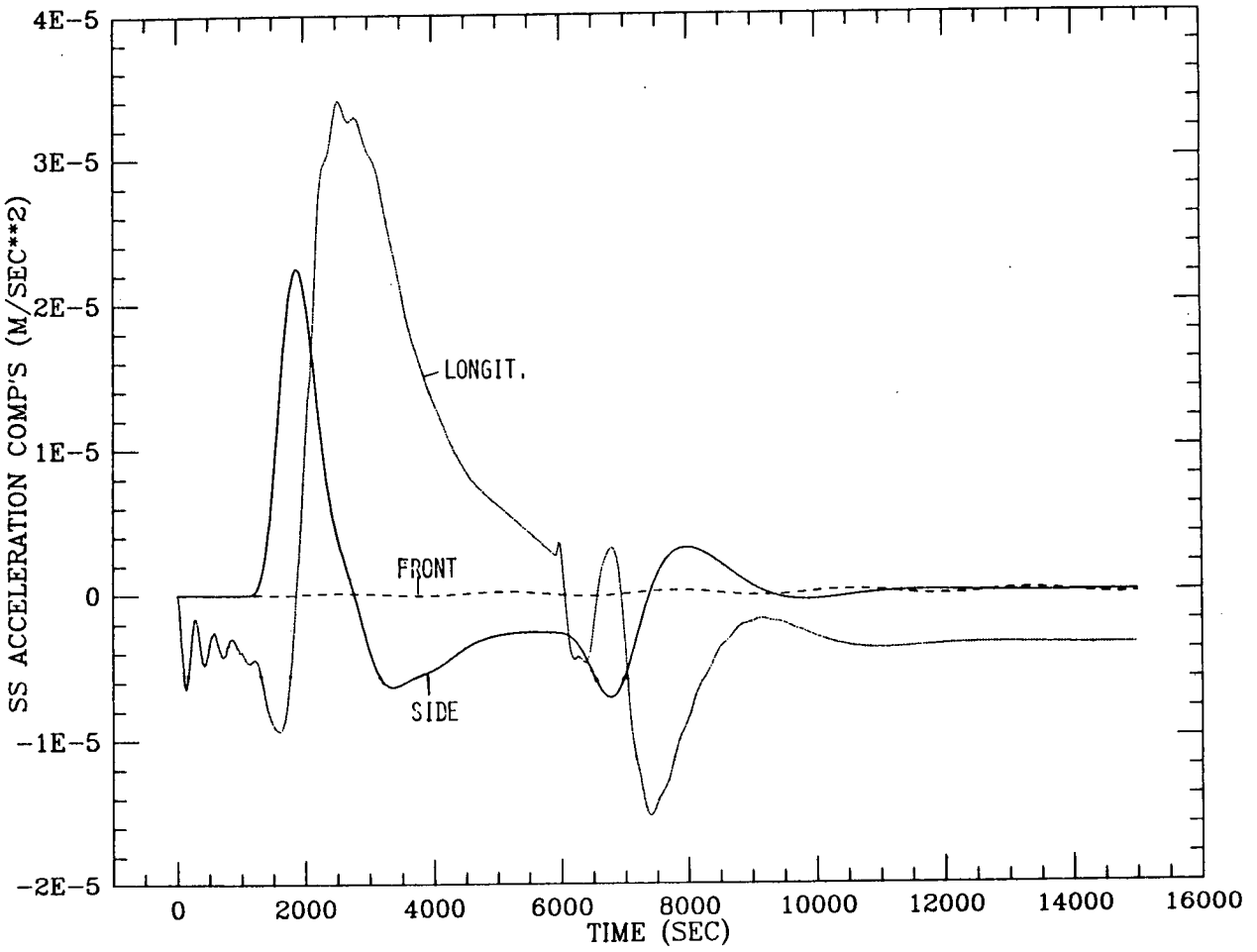
4E-5
3E-5
2E-5
1E-5
0
-1E-5
-2E-5
SS ACCELERATION COMP'S (M/SEC**2)
LONGIT.
FRONT
SIDE
0
2000
4000
6000
8000
10000
12000
14000
16000
TIME (SEC)

Figure 6j.

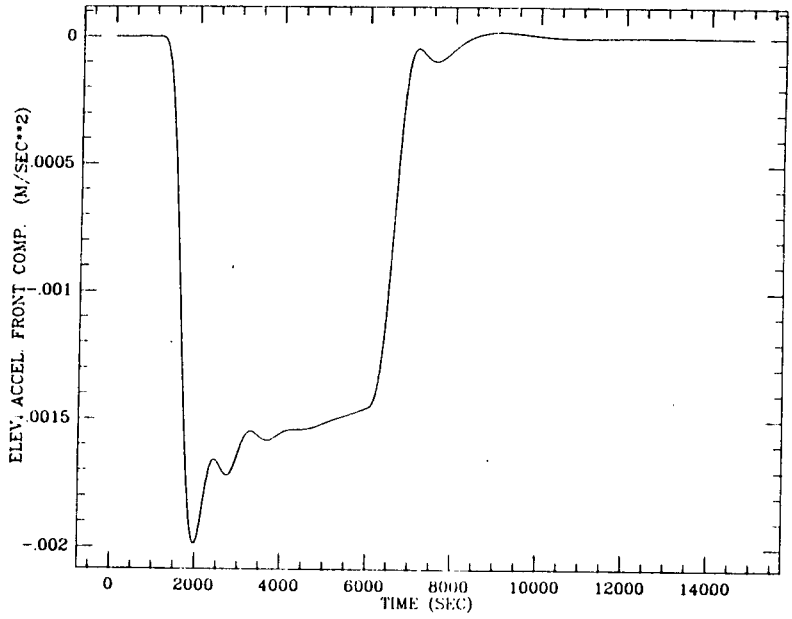

Figure 6k

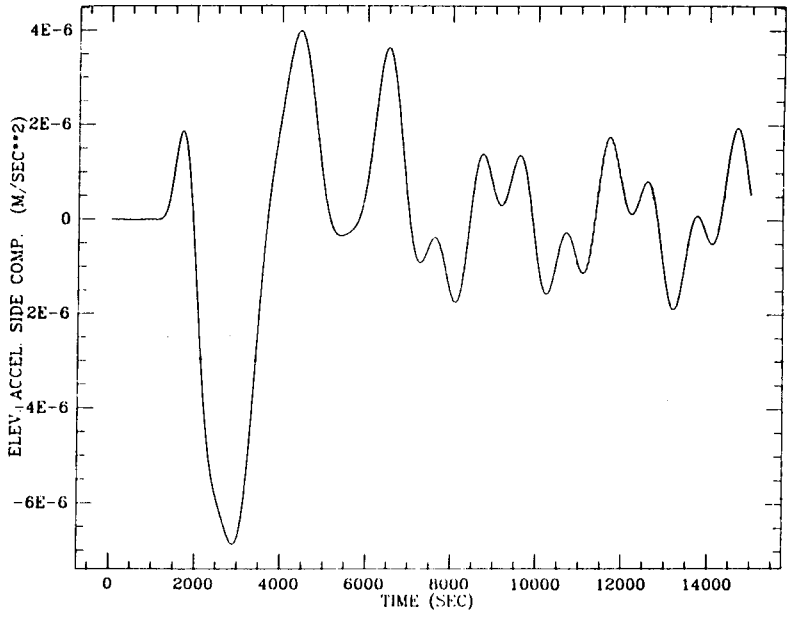

Figure 6ℓ

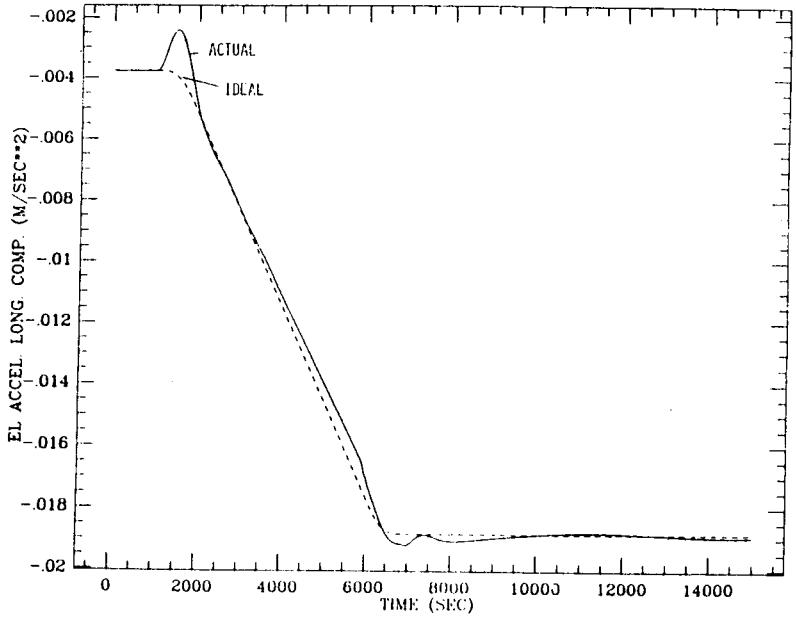

Figure 6m

The acceleration components on board the station are also slightly higher when the *MIMCL* is adopted. The acceleration components, however, are well below the 10^{-5} g limit. On the other hand the *MIMCL* is substantially faster than the *MHTCL.*

2.1.3 Concluding Remarks

The *MIM* control law has been adopted for a series of simulations runs.

Two short distance maneuvers have been simulated in accordance with the control parameters and the total travelled lengths specified for the engineering tests to be conducted on the ground.

Two simulation runs have been carried out with no external perturbations. These runs provide results which will be helpful to interpret the results of the engineering tests providing that the substantial differences between the test system and the space system are taken into account.

Two more simulation runs have been carried out by taking into account all the external perturbations. From the analysis of these latter runs we can conclude that the acceleration noise is larger than the total variation of the ideal acceleration for maneuvers up to a total travelled length of 10 m.

The *MIM* control law has also been adopted to rerun a 4 km-distance-maneuver. Two simulation runs have been carried out. One with all the external perturbations acting upon the system and one with the J_2-perturbations only. We conclude that in the case of long distance crawling maneuvers we can neglect, as a first approximation, the effects of drag and thermal perturbations if we are

interested in the time histories of the acceleration levels during the elevator's crawling.

By comparing the results obtained, under the same conditions, by adopting the *MIMCL* with those obtained by adopting the *MHTCL* we conclude that the *MIMCL* is as effective as the *MHTCL* and is substantially faster.

2.2 Modelling The Higher Harmonic Components Of Tether Vibrations

2.2.1 Preprocessor For Setting Up Initial Conditions

In the case of a multi-mass system a preprocessor is needed for providing the initial values of the integration variables once the distribution of mass of the system has been defined by the user.

The preprocessor that we developed is designed for the current version of the tethered constellation simulation program *MASTER*20 described in the next subsection. The preprocessor (and the computer code) can handle a system modelled by N lumped masses of which L are identified as platforms. At the attachment points of the tether segments to the platforms a number of $M \leq L-1$ longitudinal dampers can be arbitrarily placed by the user. The distinction between a tether bead and a platform is necessary in the case of multi-platform tethered systems because the tethers can be controlled at the attachment points to the platforms and not in between two successive tether beads.

The preprocessor reads a matrix of N rows which specify the distribution of mass of the system. The first column identifies the platforms, the tether beads and it also identifies one of the platforms as the reference platform that

coincides at the initial time with the origin of the orbiting reference frame. The ratio between two elements of the same row of the last two columns of the matrix defines what fraction of tether mass goes into that particular lumped mass. The distribution of platforms and tether lumps is therefore completely general and the user can define it without any constraint.

The preprocessor also read another large matrix that specifies the platform masses, frontal areas, orbital parameters, tethers' stiffness, damping characteristics, thermal characteristics, control parameters, type of environmental models, control options, the map of the longitudinal dampers, the integrator parameters, etc.

The user then specifies one of three options: option 1) the reference platform (e.g. the space station) coincides with the system *CM*; option 2) the reference platform coincides with the orbital center *CO* of the system; option 3) the geometry of the system is arbitrary, consequently the user specify all the lengths of the tether segments (between adjacent platforms) and the preprocessor does not adjust their lengths in order to meet the conditions specified in the previous options. In options 1 and 2, on the contrary, the length of the tether segment closer to the Earth (tether segment 1) is adjusted in order to meet the requirement associated with either option.

Under each option the preprocessor balance the centrifugal and the gravity forces (produced by a spherical gravity field) for each lumped mass, computes the natural tether length for each fractional segment of the tether (the segment of the tether between any two successive lumped mass) and the stretches of the longitudinal dampers. The preprocessor then prepares the input file in the format expected by the simulation code. The preprocessor prepares also another file, user friendly, that provides all the information related to the initial status of the

system; namely: the system's geometry, the distribution of mass, the tensions in each fractional segment of tether, the natural lengths, the stretches of the longitudinal dampers and the position of each lumped mass with respect to the rotating reference frame.

It is worth mentioning that in the current version of the preprocessor the system is assumed initially aligned with the local vertical. Initial perturbation velocities of any of the lumped masses can be very easily introduced by the user by editing the input file which is formatted and, therefore, easy to read.

2.2.2 Computer Simulation Code *MASTER*20

The computer code that we have been using thus far for the simulation of the dynamics of multi-mass tethered constellation has been illustrated throughout the previous Quarterly Reports.

In summary this computer code models the system as lumped masses connected by elastic springs. The orbit is generic. The environmental models describe accurately the *LEO* environment. They include a non-linearized gravity model with J_o and J_2 components; a Jacchia 77 model of the atmospheric density which is a function of orbital altitude and local exospheric temperature; a thermal model of the tether segments which takes into account solar illumination, *IR* radiation, Earth albedo and emitted radiation.

The integration variables are the cartesian coordinates of the lumped masses with respect to an orbiting reference frame. The computer code has several options for turning on or off the various contributions of the environmental models. The user can, for example, decide to run the program with the J_o

component only of the gravity field. It also has several options for controlling the lengths of the tether segments connecting two adjacent platforms. Longitudinal dampers, in series with the tether segments, can be placed by the user in all, some, or none of the tether segments.

The computer code has been used thus far without any tether beads. The recently upgraded version, called *MASTER*20, can handle up to 20 lumped masses which model the system (20 is an arbitrary number that can be easily expanded by changing the dimension statements into the computer code). In order to retain the capability of controlling any of the tether segments between platforms the computer code distinguishes between a platform and a tether bead. Since the reeling mechanisms are on board the platforms only the fractional segments of tethers adjacent to the platforms can be controlled. Some of the control algorithms, moreover, are fed with the positions and optionally the velocities of the platforms providing one more reason for the need of distinguishing between a platform and a tether bead. Once the geometry matrix, that is one of the user defined input of the preprocessor, is properly set up the preprocessor provides to the simulation code all the information necessary to define the geometry and the control features of the system.

The next subsection illustrates some test runs of the simulation code in which the system is modelled as 10 lumped masses (4 platforms plus 6 tether beads).

2.2.3 Test Simulation Runs

Two short simulation runs have been done: 1) to test the ability of the preprocessor in computing initial conditions for multi-mass systems and 2) to check the simulation program *MASTER*20.

The system is modelled with 10 lumped masses: 4 platforms plus 6 tether beads. The tether beads are evenly spaced in each tether segment. The lumped masses are numbered sequentially from 1 to 10 starting from the bottom. The platforms are, therefore, as follows: lumped mass 1 for the lower platform, 4 for the space station, 7 for the elevator and 10 for the upper platform (see Figure 7). Three longitudinal dampers, tuned to the bobbing frequencies of the associated tether segments, are in series with the three tether segments. No environmental perturbation is acting upon the system and the gravity field is spherical.

In the first test run we used option 1 of the preprocessor which implies that the reference platform, namely the space station, is placed at the system *CM*. It is important to remember that the reference platform coincides, at time equal to zero, with the origin of the reference frame and that the initial orbital velocity of the system is assumed to be equal to that one of the orbiting reference frame unless provisions are taken by the user. The *CO*, where the gravity and centrifugal forces cancel out, does not coincide with the *CM* in a long system such as a tethered system. Consequently the system does not follow a circular orbit when the initial position and velocity of the system *CM* coincide with those of the rotating reference frame that follows the circular orbit of a point mass at that altitude.

The effect, described above, clearly appears in Figures 8a-8d. The orbit of the system is getting slightly elliptical and the initial position of the *CM* is the

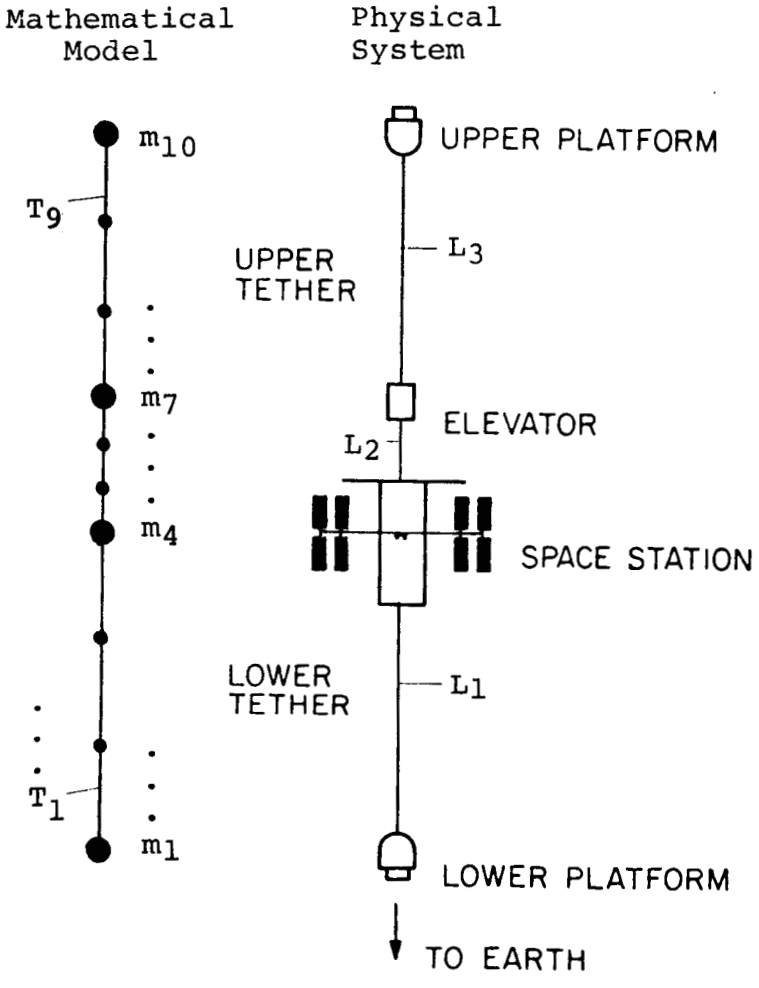
Mathematical Model
Physical System
m_{10}
T_9
m_7
m_4
T_1
m_1
UPPER PLATFORM
UPPER TETHER
L_3
ELEVATOR
L_2
SPACE STATION
LOWER TETHER
L_1
LOWER PLATFORM
TO EARTH

Figure 7.

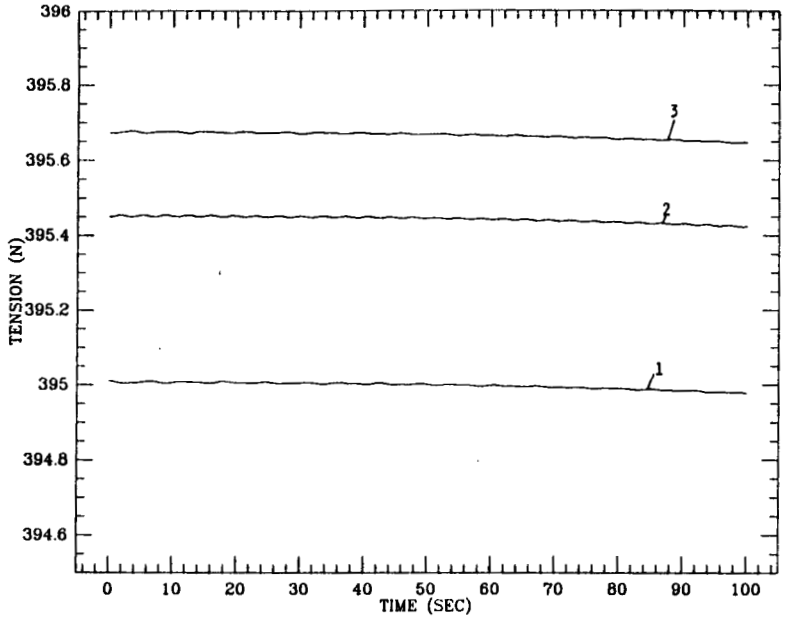

Figure 8a

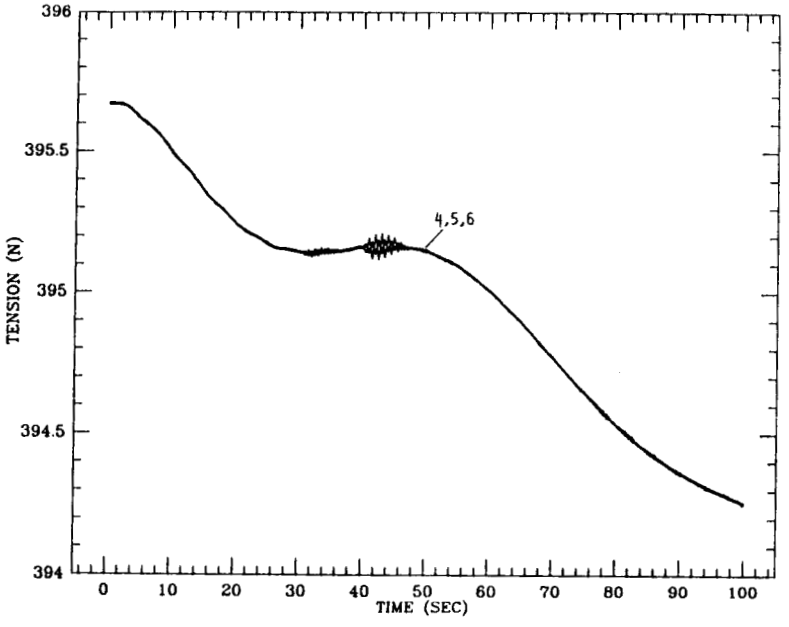

Figure 8b

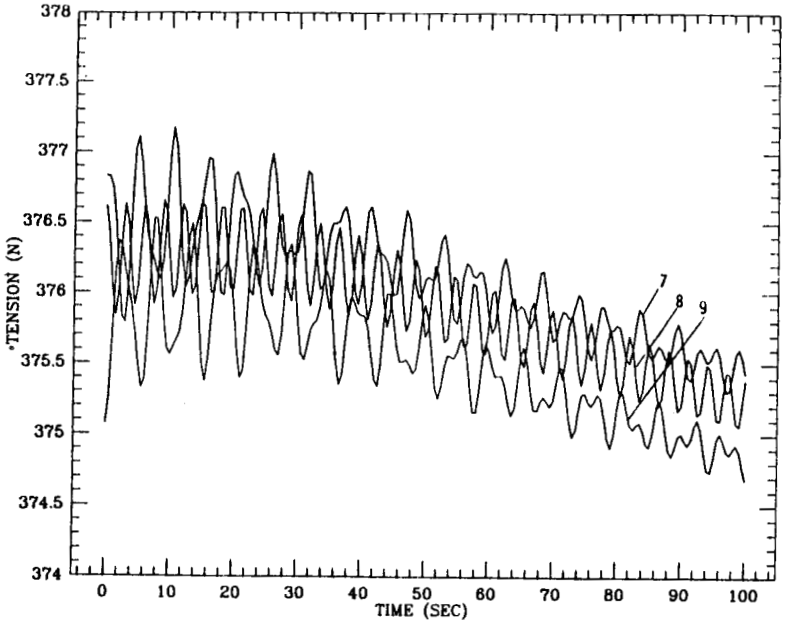

Figure 8c

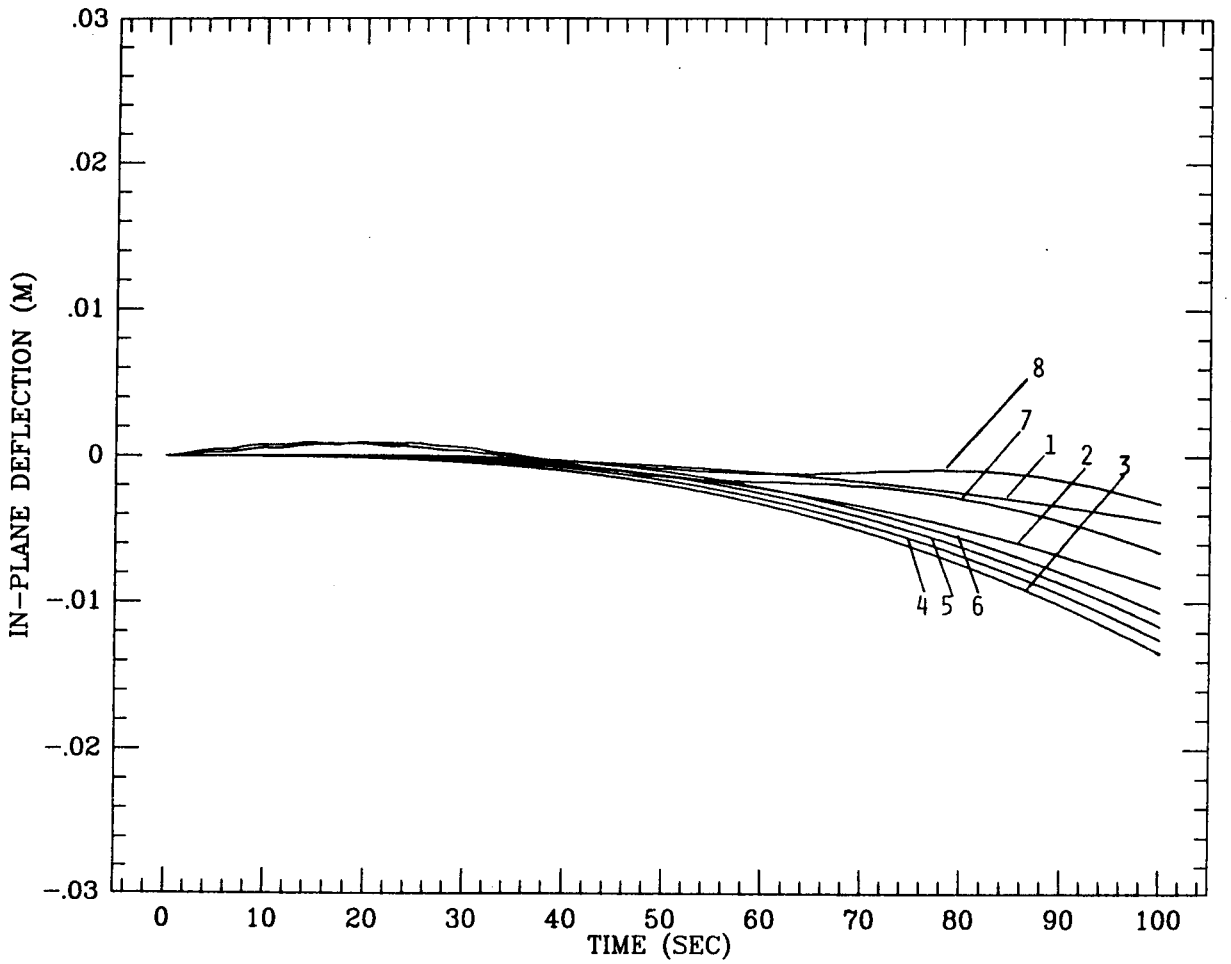
.03
.02
.01
0
-.01
-.02
-.03
IN-PLANE DEFLECTION (M)
0
10
20
30
40
50
60
70
80
90
100
TIME (SEC)
8
7
1
2
3
4
5
6

Figure 8d.

apogee of the orbit. The tether segments are initially slightly stretched because of the effect mentioned above and the higher harmonic of the longitudinal oscillations are excited. Figures 8a and 8c show the tether tensions as follows: tensions 1, 2 and 3 are associated with tether segment 1; tensions 4, 5 and 6 with tether segment 2; and tensions 7, 8 and 9 with tether segment 3. Figure 8d shows the in-plane component of the lateral deflections of the inner-masses (platforms and tether beads) with respect to the end-masses. The higher harmonic components and the low frequency component (that looks like a drift over such a short time frame) are clearly evident in the three plots.

For the second simulation run we made use of option 2 of the preprocessor. Option 2 asks for the reference platform (i.e. the space station) to be placed initially at the system *CO*. In this case the gravity and centrifugal forces are balanced at the orbital rate and at the altitude of the orbiting reference frame and the system follows a steady-state circular orbit in absence of external perturbations. The tensions and the deflections are expected to maintain their initial values (within the accuracy selected for the integration) if the simulation code works properly. This indeed happens and is shown clearly in Figures 9a-9d. The low frequency "drift" disappears and the tensions are very close to constant values. The in-plane deflections are well within the relative accuracy of the integrator which has been set to 10^{-5}.

The CPU time for running the 10-lumped-mass system is substantially long. On a MircoVax and with the accuracy indicated above (when studying the gravity levels on board the platforms, however, the accuracy should be increased) the ratio CPU Time/Real Time is equal to 2.5/1.

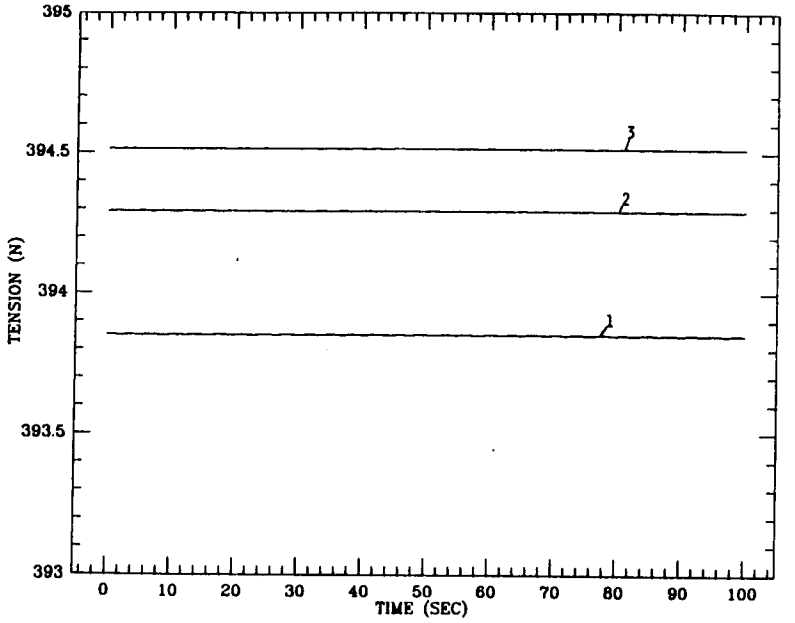

Figure 9a

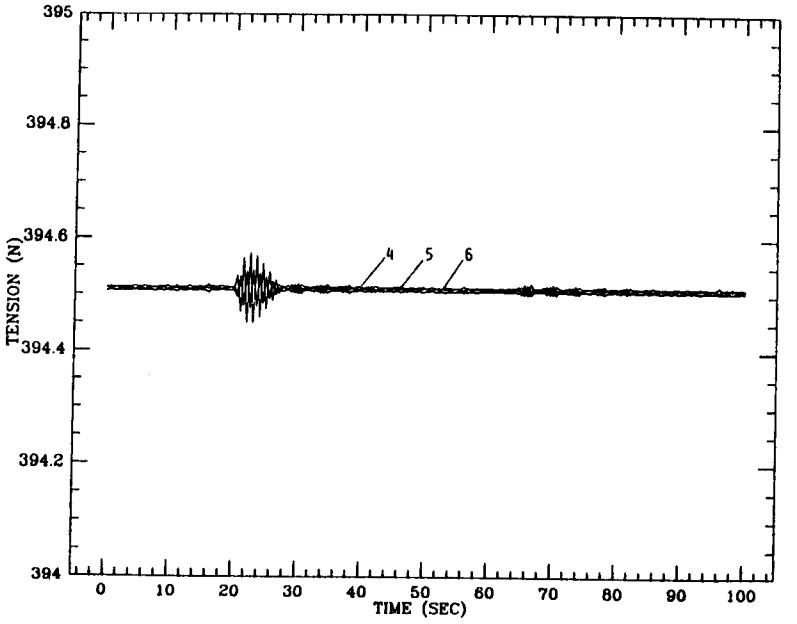

Figure 9b

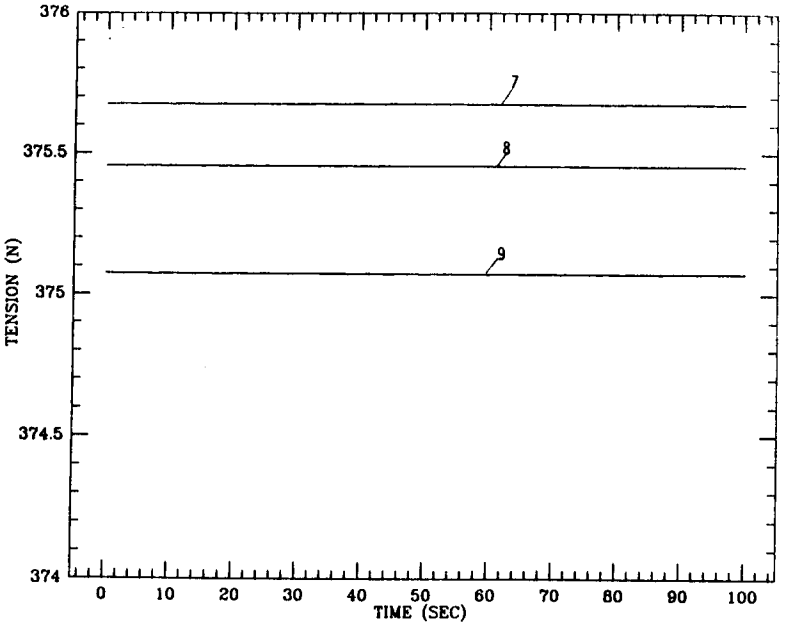

Figure 9c

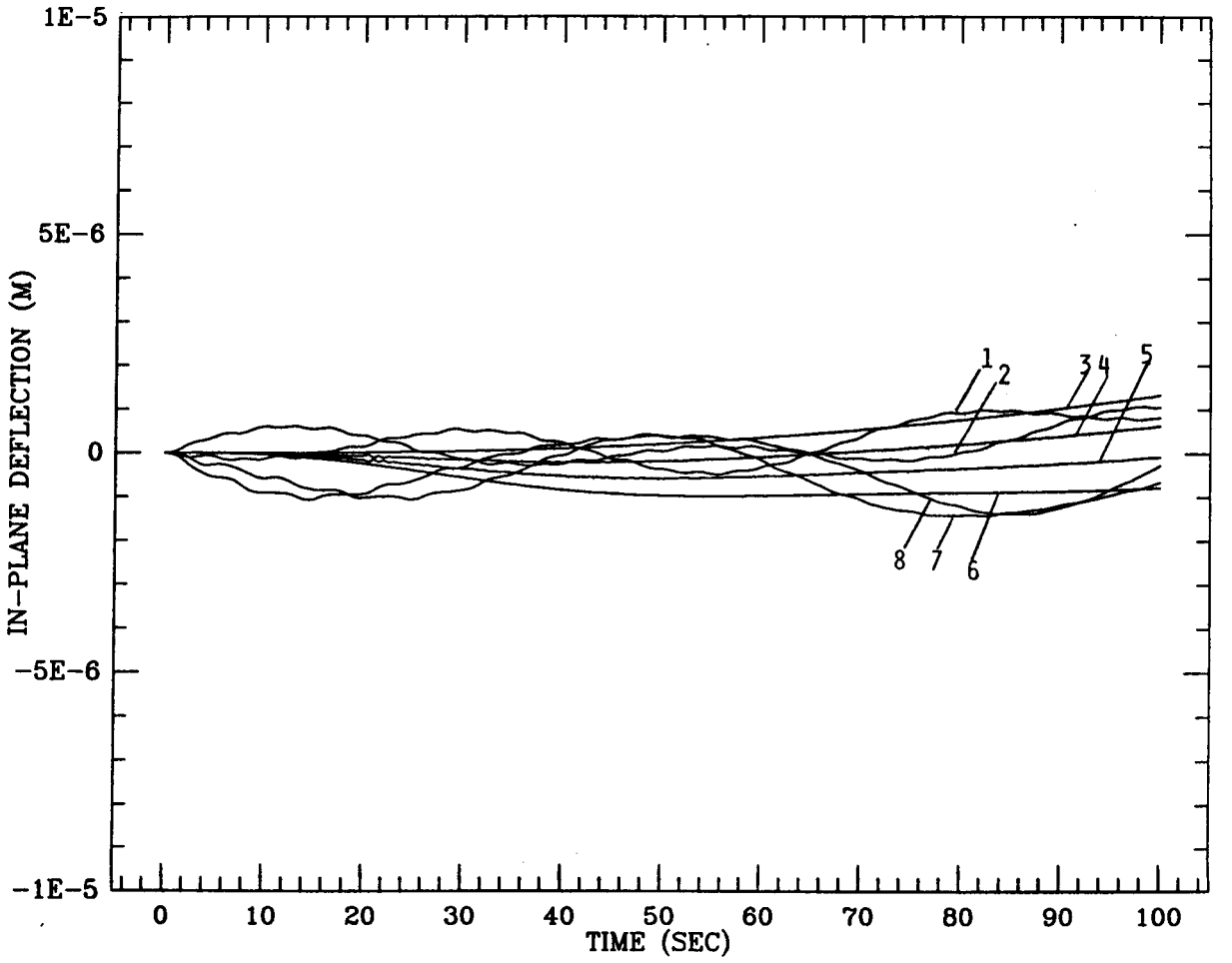
1E-5
5E-6
0
-5E-6
-1E-5
IN-PLANE DEFLECTION (M)
0
10
20
30
40
50
60
70
80
90
100
TIME (SEC)
1
2
3
4
5
6
7
8

Figure 9d.

2.2.4 Concluding Remarks

The computer code for simulating the dynamics of multi-mass tethered systems has been upgraded to handle a system of N lumped masses of which L are platforms and with $M \leq L-1$ longitudinal dampers. A user-friendly preprocessor has also been developed for computing the initial conditions of a complex multi-mass system formed by platforms, tether beads and longitudinal dampers. The preprocessor has options tailored to the dynamics simulation of micro-gravity systems. These options have been exercised in two short runs of the upgraded computer code *MASTER*20 aimed at testing this upgraded version of the code.

2.3 Tether Applications Simulation Working Group Support By G.E. Gullahorn

2.3.1 Introduction

SAO is working in support of the Tether Applications Simulation Working Group. Three primary tasks are currently being worked. First, an updated catalog of tether simulators is being prepared on the basis of a circulated questionnaire. Second, a catalog of "analytic solutions," i.e. precisely computable solutions in restricted or limiting cases, is being prepared. Third, a set of test cases for inter-comparison of simulation programs has been prepared; sample results from SKYHOOK and other simulators have been obtained and will be compared. A further task shall be to define suggested environmental models for inclusion in current and future simulators.

2.3.2 Questionnaire Subcommittee

The questionnaire appended to Quarterly Report No. 9 was circulated to some 350 people with an indicated interest in tether dynamics. Eighteen responses have been received. A number of other people requested copies of the resulting report. A presentation is being prepared for the Second International Conference on Tethers in Space (Venice, Italy, 1987 October 4-8), at a workshop organized by the Working Group. This presentation will be included in the next Quarterly Report

2.3.3 Analytic Solutions Subcommittee

Little work on the overall cataloging of analytic solutions has been done in this reporting period. One case of practical interest, the longitudinal response of a tethered system taking into account gravity gradient, a finite end mass, and continuous, damped, elastic tether, has been explored under other contracts and pro bono. The propogation of impulsive disturbances along the tether (e.g. generated by operations aboard the Shuttle) and the response on the satellite has been solved in closed form for the undamped case, and in a form requiring some numerical work in the damped case. The current contract has partially supported preparation of a paper to be presented at the Venice conference. A copy of this paper is in Appendix A.

2.3.4 Simulator Test Cases

A set of four test cases designed to elicit a variety of different behaviors has been devised. They are designated A to D. Two of these cases (A and C) involve satellite attitude dynamics; the other two are for point mass satellites. A mailing was made to a number of people possessing simulators: (1) specification of the four cases, (2) a matrix showing the expected phenomena for each case, (3) a "data base" giving values for system and environment parameters, and (4) a requested output format. This mailing, with its cover letter, is reproduced in Appendix A.

Responses were received from P. Bainum and A. Banerjee for cases B and D (those not involving attitude dynamics). D. Lang responded for all four cases.

We are in the process of performing SKYHOOK simulations of the test cases at SAO. Cases B and D have been completed. Cases A and C (the attitude dynamics cases) have been hindered in that the attitude dynamics version of SKYHOOK has not been used in some five years, and the existing version included some modifications for special purposes (e.g. a "hardwired" thruster) which had to be removed. Additionally, the SKYHOOK input format of rotation related quantities is not fully documented as to coordinate systems and units, nor is the DUMBEL preprocessor. Effort is proceeding to perform suitable runs for cases A and C.

A presentation is being prepared for the Venice conference. Comparisons of the four sets of results for the cases B and D will be made. Presuming satisfactory completion of the SAO results for A and C, these also will be presented. A copy of this presentation will be appended to the next Quarterley report.

2.3.5 Concluding Remarks

Responses to the catalog questionnaire have been received and are being consolidated. A set of four simulator test cases has been prepared and circulated to selected simulator operators. Results have been received from several simulators; these will be compared. Each of these activities will result in a presentation at the Second International Conference on Tethers in Space in Venice. In addition, a contributed paper on a particular analytic solution in tether dynamics will be given in Venice.

3.0 PROBLEMS ENCOUNTERED DURING REPORTING PERIOD

None

4.0 ACTIVITY PLANNED FOR NEXT REPORTING PERIOD

The dynamics of the 4-platform system will be simulated by taking into account the higher order harmonics of the longitudinal and lateral oscillations of the tether segments. The investigation of the isolation augmentation between the space station and the elevator will also be initiated.

SAO will present a catalog of tether simulations at the Second International Conference on Tethers in Space in Venice. Further SAO results on test cases will be generated, and comparisons made between SAO results and those from other institutions; these comparisons will be presented in Venice. A contributed paper detailing a particular analytic solution will also be given at Venice. Work will continue on the catalog of analytic solutions.

Documents in support of Tether Applications Simulation Working group